Photocathode developments for robust PICOSEC Micromegas precise-timing detectors

MARTA LISOWSKA

ON BEHALF OF THE CERN GAS DETECTORS DEVELOPMENT TEAM AND THE PICOSEC MICROMEGAS COLLABORATION

10 DECEMBER 2024

GDD
Gas Detectors Development Group

CERN EP R&D PICOSEC Micromegas

DRD1

PICOSEC Micromegas

Detector concept

- **PICOSEC Micromegas:** a gaseous detector aiming at achieving **a time resolution of tens of picoseconds** for MIPs

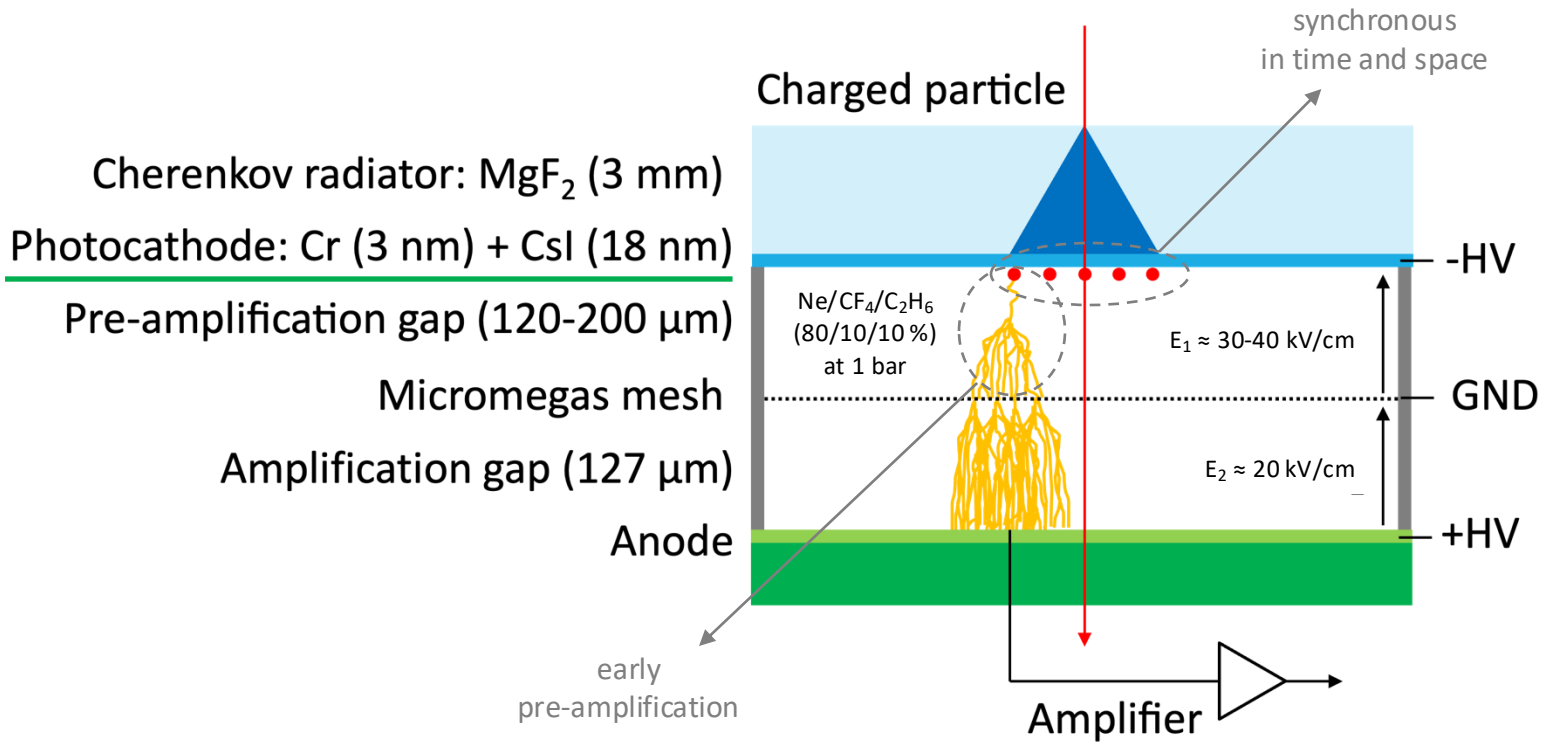

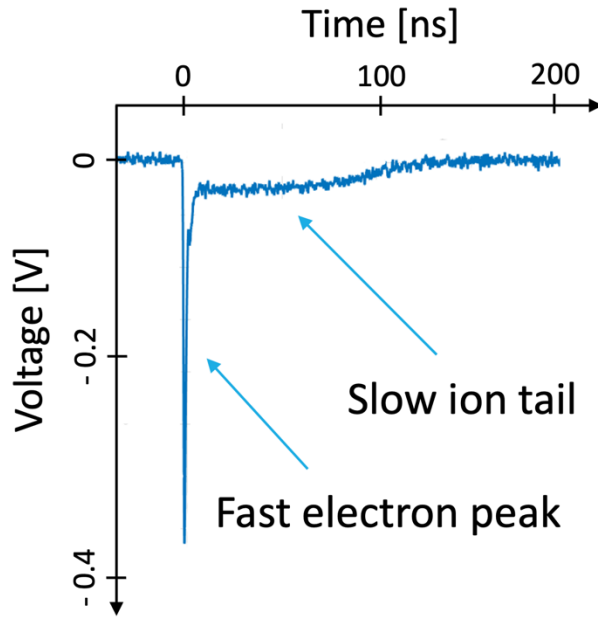

J. Bortfeldt et al., NIM A 903 (2018) 317

- First single-pad prototypes achieved a time resolution of σ = 24 ps → Potential for further improvement and performance enhancement

PICOSEC Micromegas

Single-pad prototype

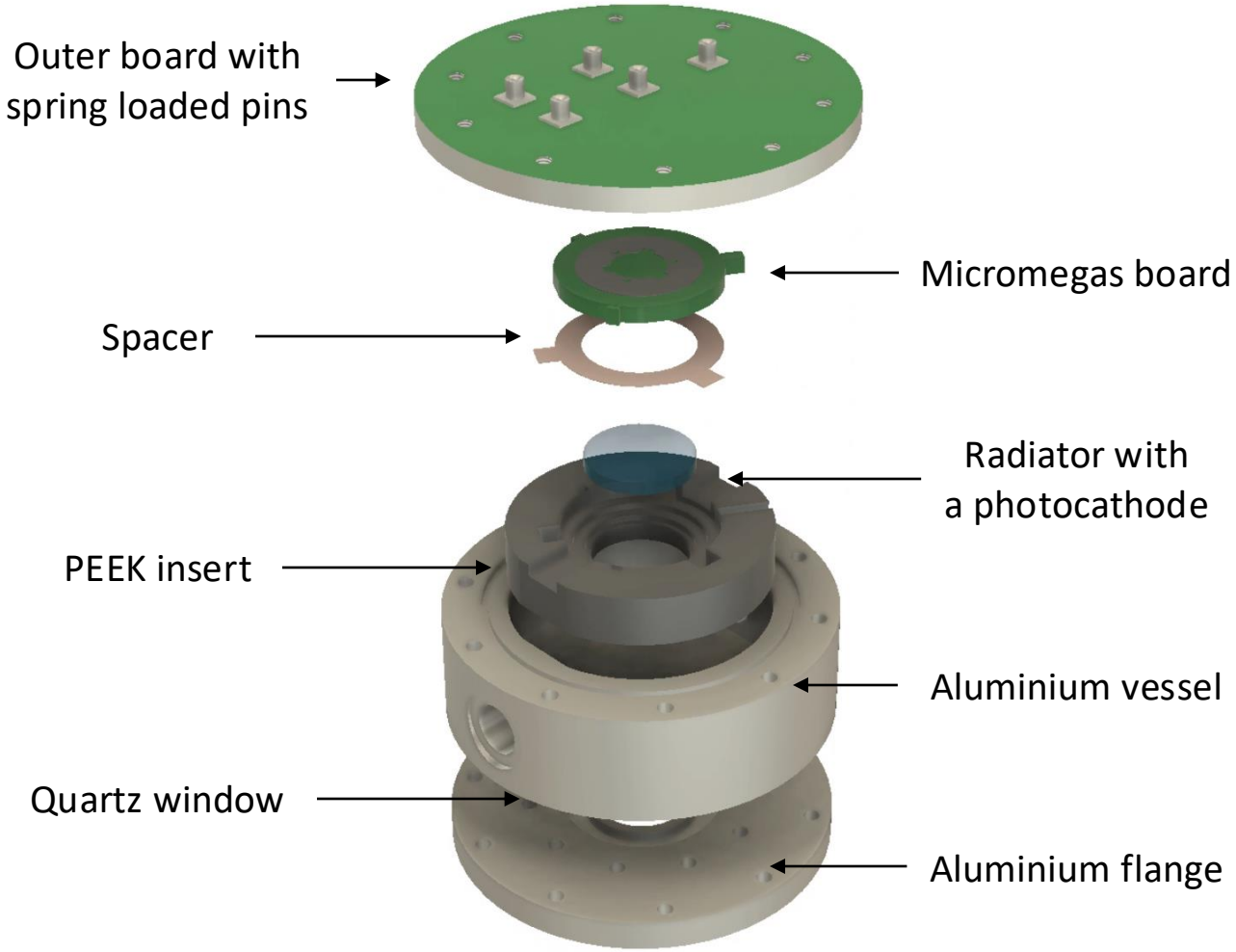

PICOSEC amplifier cards

PICOSEC amplifier design:
A. Utrobičić, et al. JINST 18 (2023) C07012
based on the RF pulse amplifier:
C. Hoarau, et al., JINST 16 (2021) T04005

LeCroy WR8104 oscilloscope

PICOSEC Micromegas

Developments towards applicable detector

- **Objective:** Robust tileable multi-channel detector modules for large-area coverage

- **Detector optimisation:**

  gaps thickness, fields settings, operating gas

- **Stability and robustness:**

  resistive Micromegas, **robust photocathodes**

- **Large area coverage:**

  100-channel prototypes, tileable modules

- **Scalable electronics:**

  dedicated amplifiers, multi-channel digitisers

Single-pad prototypes to understand detector behaviour, more cost-effective and practical

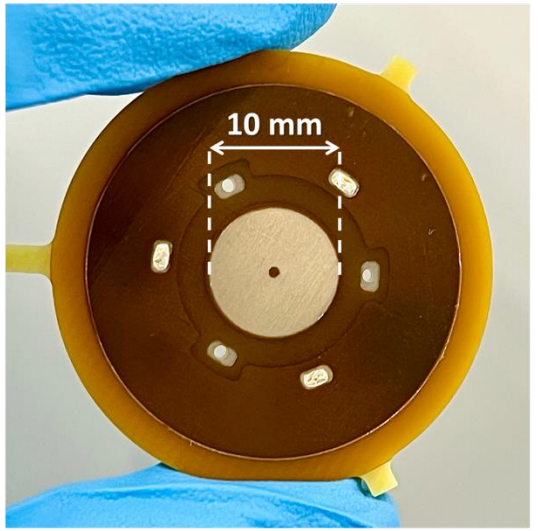

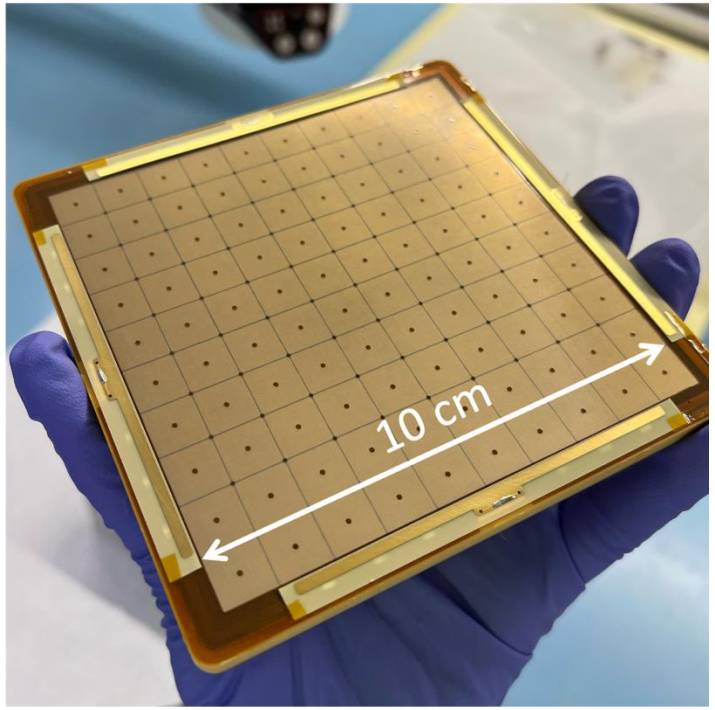

PICOSEC photocathodes

Component parts

- **Radiator:** 3 mm MgF_2

  - thickness influences the UV photon production and the Cherenkov cone size

- **Interfacial conductive layer:** 3 nm Cr

  - provide a contact for the HV to the photocathode

  - mitigate charging-up effects and voltage drops under high-rate conditions

  - Ti as an alternative

- **Semi-transparent photocathode:** 18 nm CsI

  - excellent time resolution but not a robust solution

  - dependance between the time resolution and number of photoelectrons N_{PE}:

$$\sigma_{\mathrm{MIP}} = \frac{\sigma_{\mathrm{SPE}}}{\sqrt{N_{PE}}} \quad \rightarrow \quad \sigma_{\mathrm{SPE}} = \mathrm{const} \quad \rightarrow \quad \sigma_{\mathrm{MIP}} \backsim \frac{1}{\sqrt{N_{\mathrm{PE}}}}$$

where: σ_{MIP} - time resolution for MIPs, σ_{SPE} - time resolution for single photoelectrons (SPE)

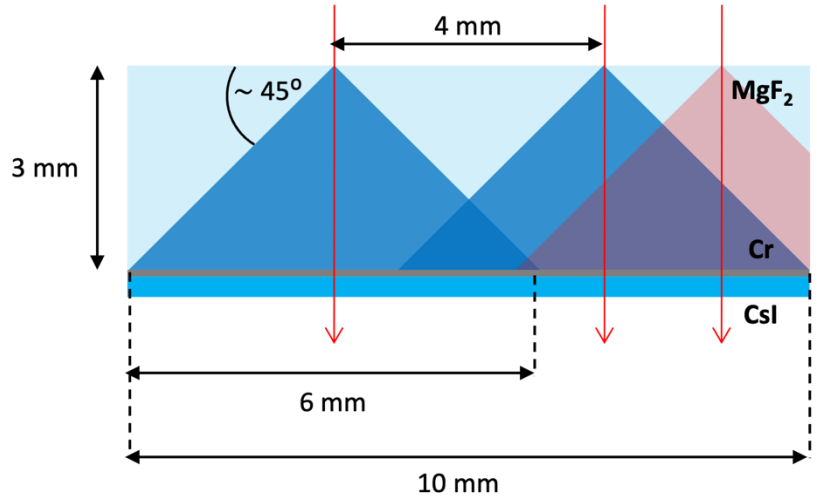

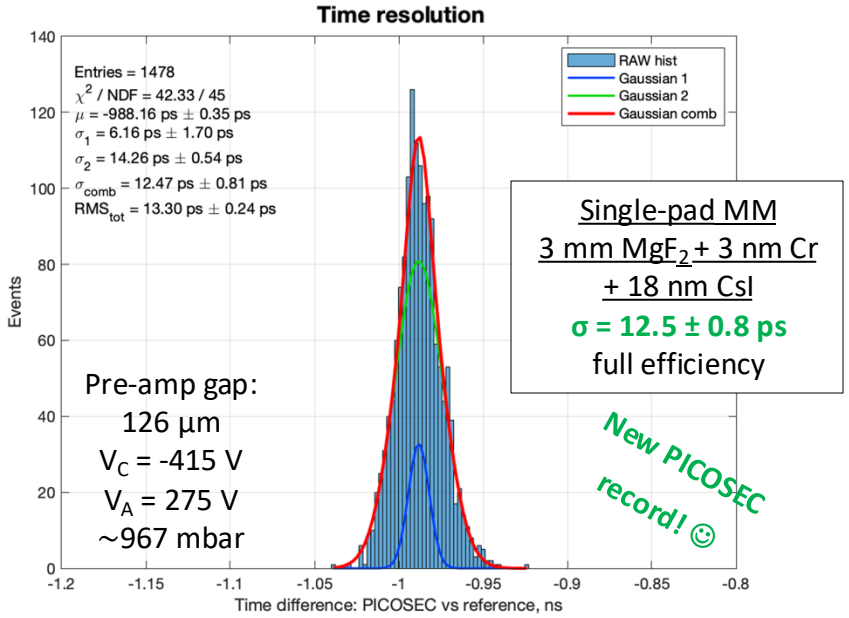

A. Utrobičić et al., arXiv:2406.05657

PICOSEC photocathodes

CsI photocathode and the alternatives

- **Single-pad prototype:**

  3 mm MgF_2 + 3 nm Cr + 18 nm CsI photocathode

  + high QE with N_{PE} exceeding 12 per MIP[1],

  thereby contributing to its excellent time resolution

  - can be damaged by ion back flow (IBF), discharges

  - sensitive to humidity (during assembly)

- Need to search for **alternative materials**:

  → Diamond-Like Carbon (DLC)

  → Boron Carbide (B_4C)

  → Nanodiamonds

  → Carbon nano-structures

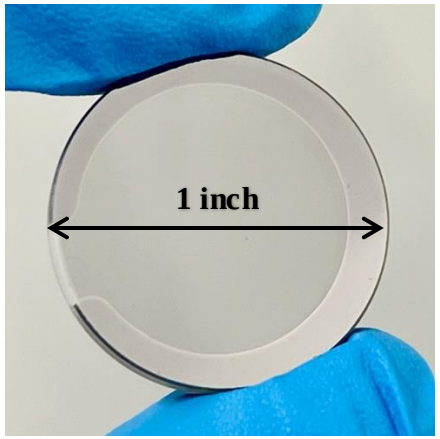

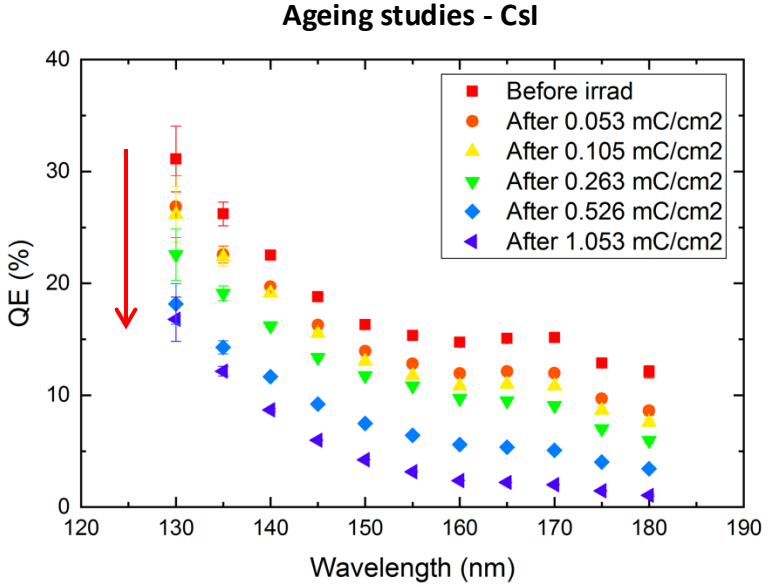

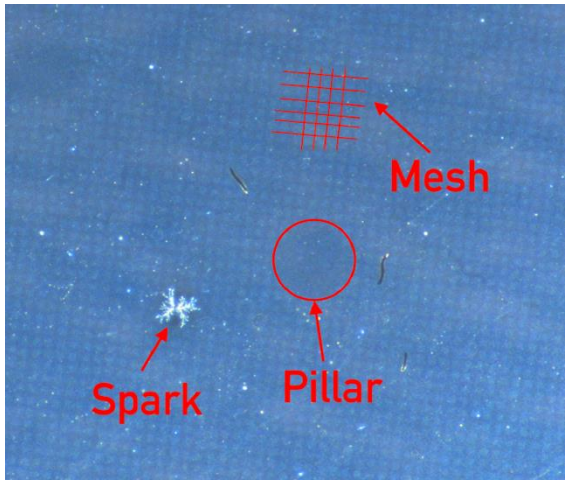

CsI photocathode damaged by IBF

L. Sohl, PhD dissertation

CsI photocathode after air exposure

[1] *J. Bortfeldt et al., NIM A 903 (2018) 317*

Experimental methodology

ASSET setup overview

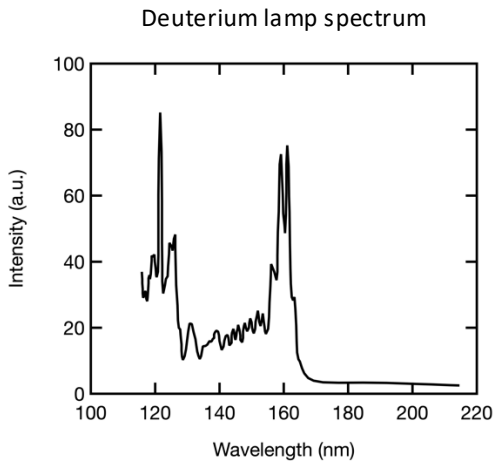

Gate valve
Gate valve
PMT movement
Irradiation mode
Top CsI PMT
Reflective measurement sample
Extraction grid
Gas mixture:
Ar/CO_2 (70/30 %)
Sample mounting glovebox
Linear sample movement
Collimator
Deuterium lamp
Multiplication wires
X-ray tube
Collimating chamber
Transmission measurement sample
Monochromator
Beam splitter
Bottom CsI PMT
Turbomolecular pump

M. Lisowska, MSc thesis

Experimental methodology

Measurements with particle beams

- **R&D activities:** From simulations and design, through production and assembly, to measurements and analysis

- **Objective of the test beam campaigns:** to measure the time resolution of the detectors assembled in various configurations

- **Beam type:** CERN SPS H4 beam line, 150 GeV/c muons

- **Experimental setup:** tracking/timing/triggering telescope

  → Triple-GEM detectors for particle tracking $\sigma_{GEM} < 80$ µm

  → MCP-PMT for timing reference and DAQ trigger $\sigma_{MCP} \approx 6$ ps

  → PICOSEC Micromegas (MM) detectors under test

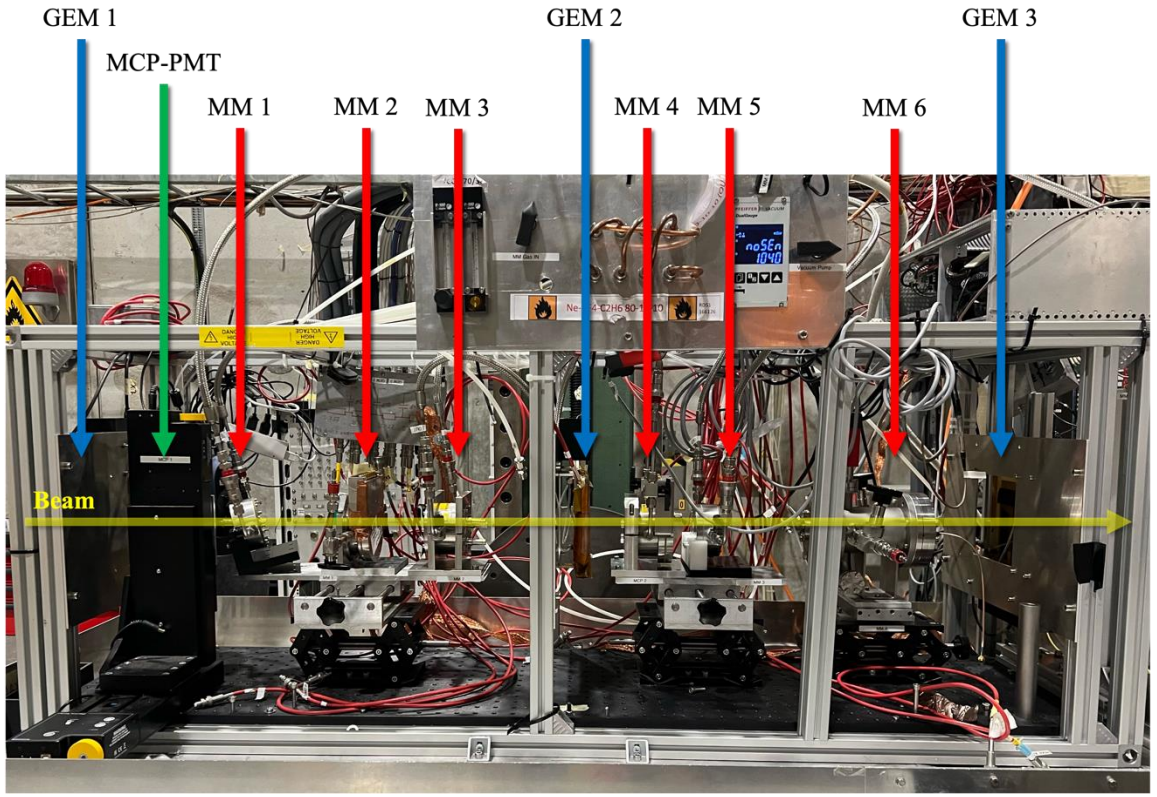

Experimental methodology

Number of photoelectrons

- Perform single photoelectron (SPE) measurements[1] using a UV light-emitting diode (LED) and multiple photoelectron measurements using a MIP beam
- Determine the maximum amplitude for each waveform
- Plot a histogram of all maximum amplitudes for both cases
- Fit the noise component using a Gaussian, while the signal component using a Pólya
- Divide the mean amplitude of the MIP V_{MIP} by the mean amplitude of the SPE V_{SPE} to obtain N_{PE} for a given photocathode:

$$N_{PE} = \frac{V_{MIP}}{V_{SPE}}$$

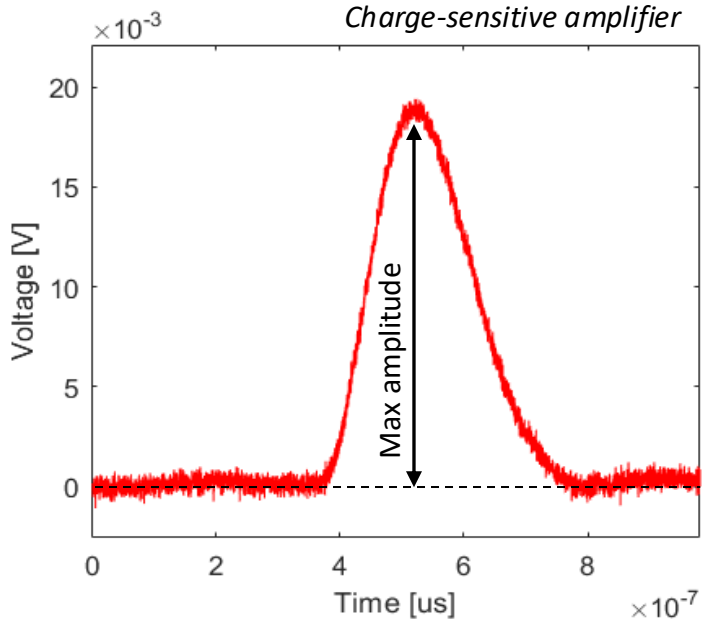

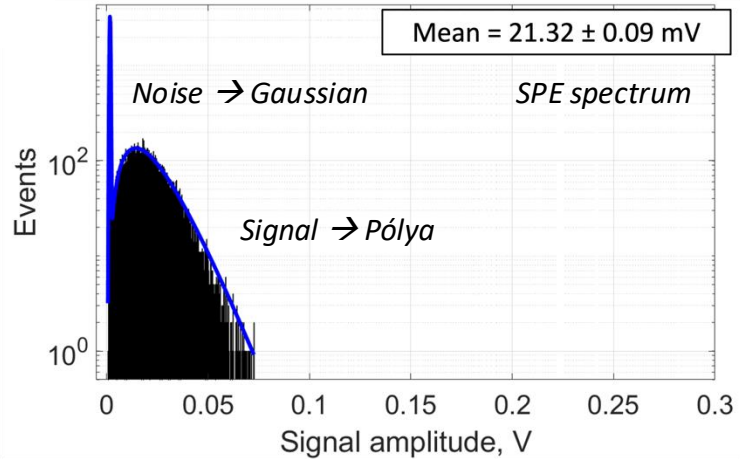

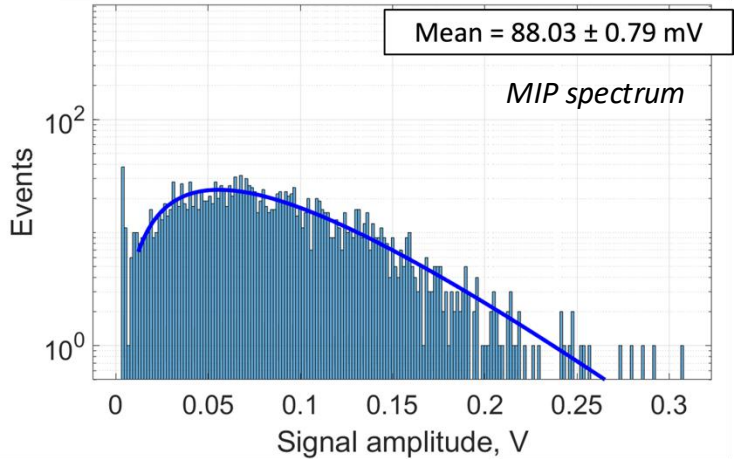

[1]Extraction of one photoelectron at a time was ensured by setting the LED to a low rate and monitoring the waveforms on the oscilloscope to confirm that events did not overlap but were well separated in time

M. Lisowska et al., arXiv:2407.09953

Photocathode characterisation

Diamond-Like Carbon – production

Possibility to deposit DLC photocathodes at the CERN MPT workshop

- DLC deposited at USTC showed good performance and robustness
- Depositions using a magnetron sputtering technique at the CERN MPT workshop to explore capabilities
- Two deposition campaigns: DLC photocathodes done with layer thicknesses ranging from 1.5 nm to 100 nm

Pulsed DC magnetron vacuum deposition machine

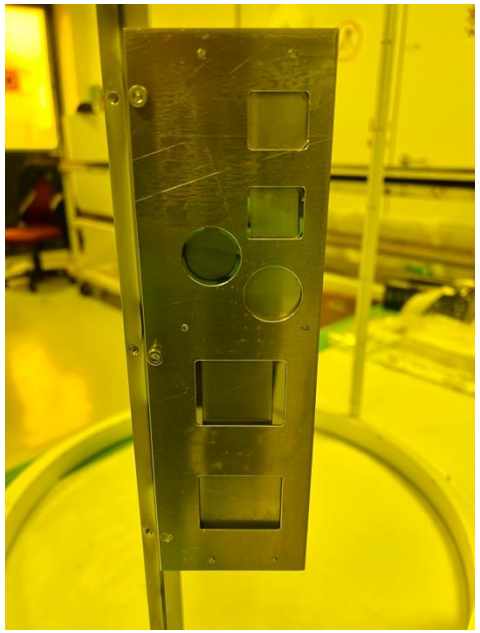

Samples inside the holder with different sizes and masks

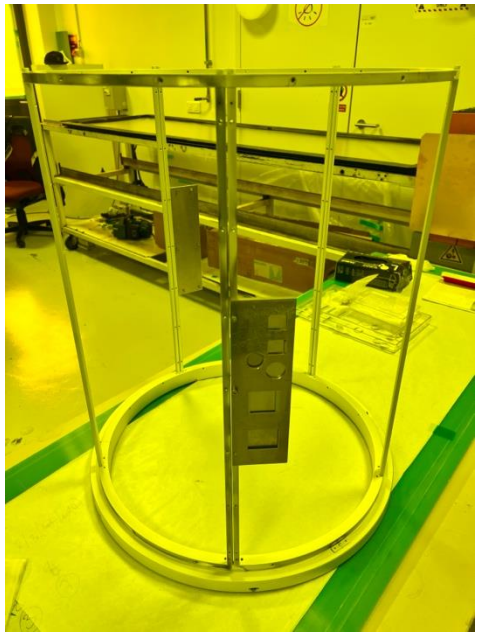

Holders with samples attached to the drum

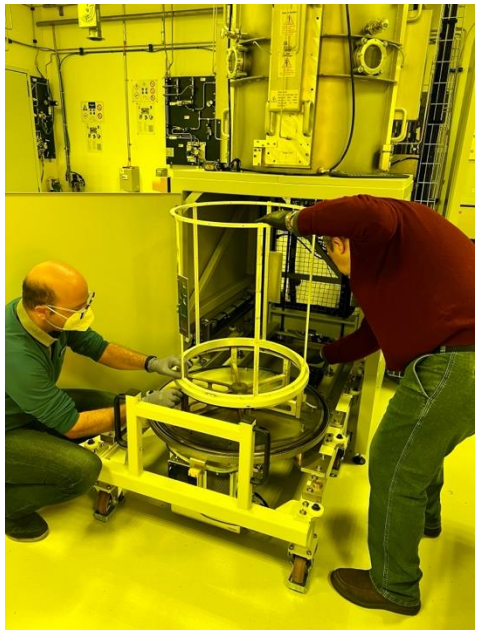

Loading the drum into the chamber

Huge thanks to Serge, Rui, Gianfranco, Givi, Louise Miranda and Thomas for the opportunity to do the deposition as well as all the help during the procedure!

Details on the machine: MPGD School 2024, R. de Oliveira: link

Photocathode characterisation

Diamond-Like Carbon – laboratory measurements

Successful deposition of DLC of different layer thickness

- **Transparency** measurements in the UV-VIS range obtained with a spectrophotometer
- The data demonstrate a correlation between the estimated thicknesses and the measured transparency
- **Surface resistivity** measurements performed using a picoammeter to confirm if the estimated thicknesses follow the expected trend
- Higher resistivity for DLC on MgF_2 than DLC on glass → DLC on MgF_2 is thinner, potentially due to the lower adhesion of the crystal

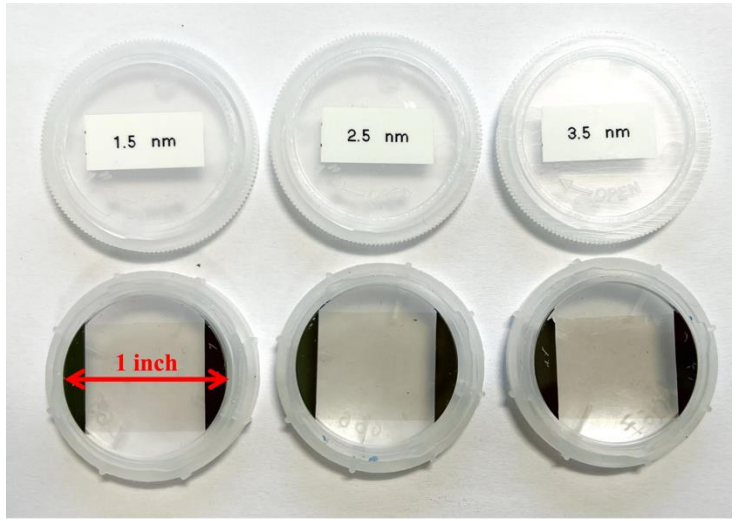

DLC photocathodes with varying layer thicknesses

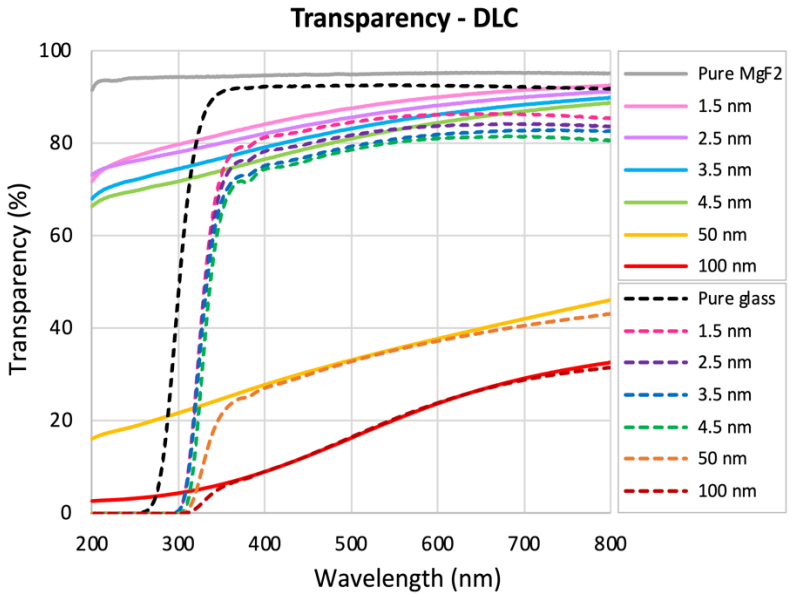

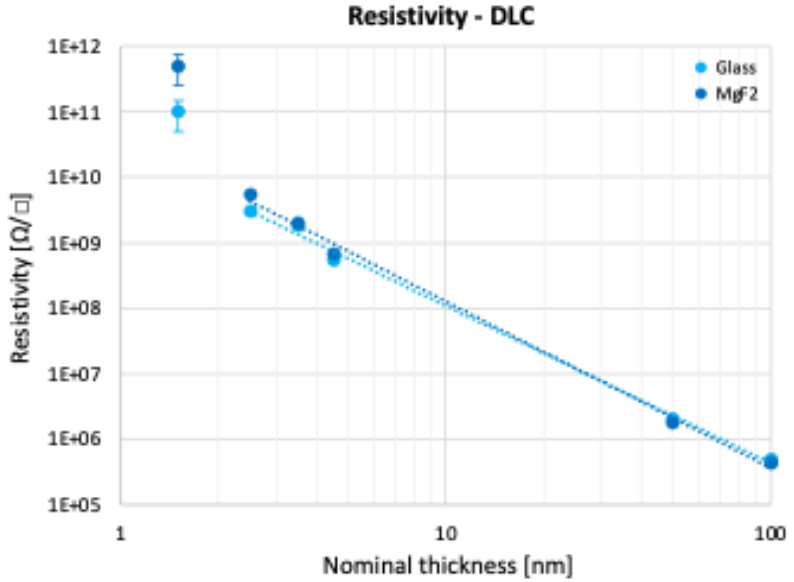

M. Lisowska et al., arXiv:2407.09953

Photocathode characterisation

Diamond-Like Carbon – particle beam measurements

- DLC photocathodes, ranging in thickness from 1.5 nm to 3.5 nm, were characterised during particle beam measurements
- **Detector with a 1.5 nm DLC** deposited directly on the radiator, **exhibited σ = 31.9 ± 1.3 ps**; thicker samples ~4 ps worse resolution
- Evaluation of the samples including 3 nm Cr interfacial layer showed a transparency decrease by ~30% and a 2 ps worse time resolution
- To enhance UV photon production, a **5 mm MgF_2 radiator** with a 2.5 nm DLC was tested

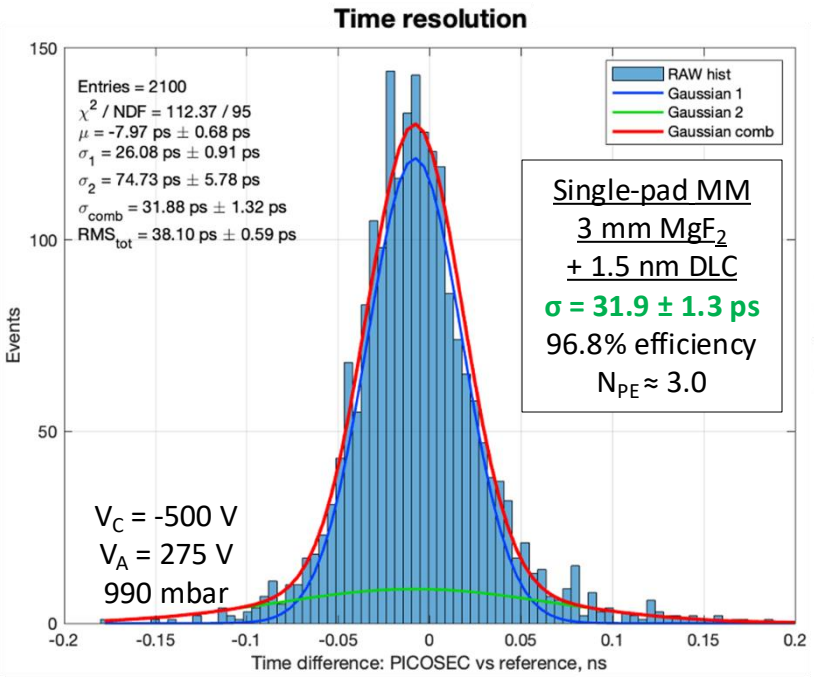

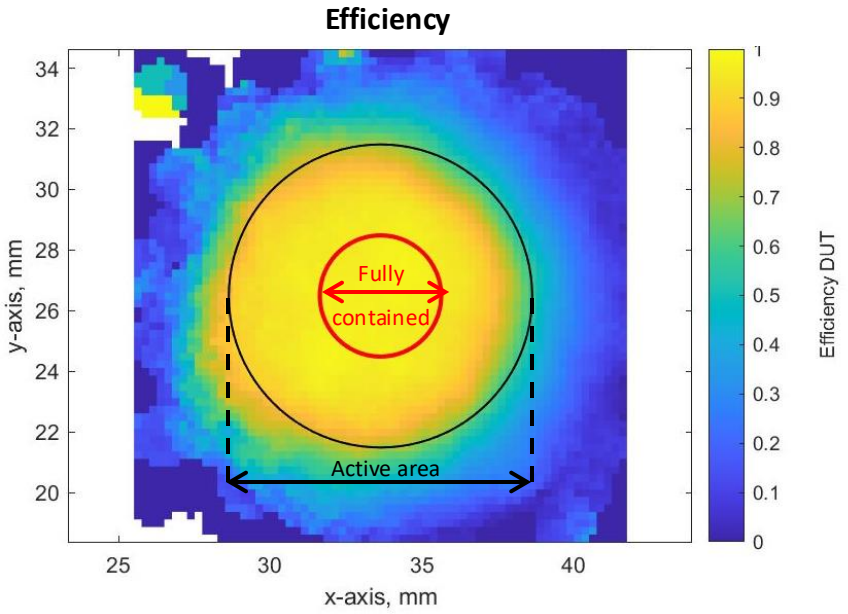

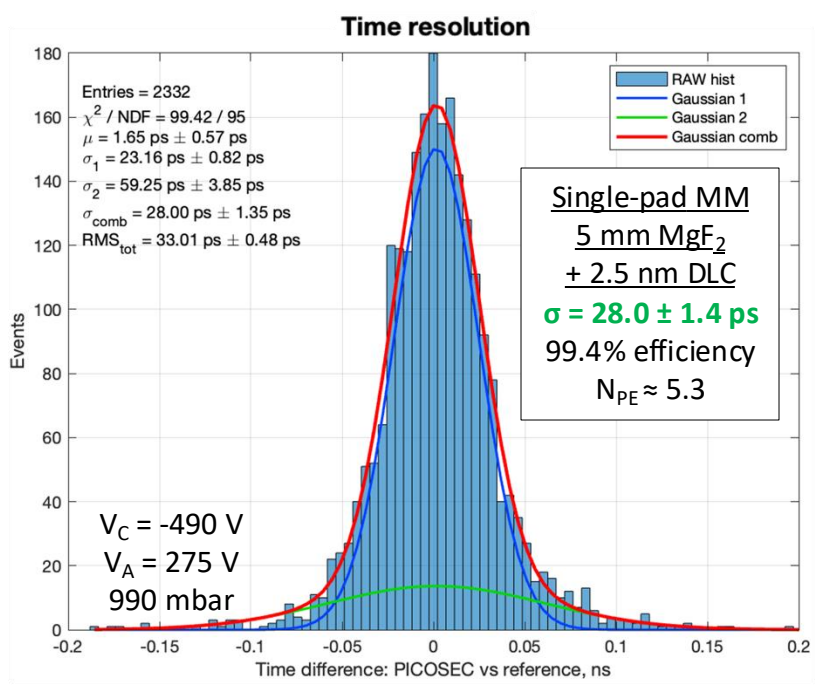

Photocathode characterisation

Boron Carbide

- B_4C photocathodes deposited at CEA-Saclay and ESS showed promising results
- Samples of 3 mm MgF_2 + 3 nm Cr + B_4C from 7.5 nm to 15 nm showed transparency from 40% to 20% (@180 nm)
- **Detector with a 9 nm B_4C** and a 3 nm Cr interfacial layer **exhibited σ = 34.5 ± 1.5 ps**
- Thicker samples showed up to ~10 ps worse resolution

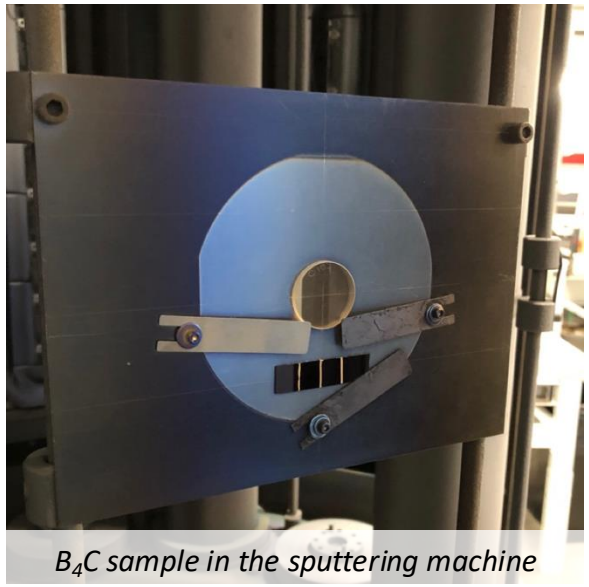

B_4C sample in the sputtering machine

C.-C. Lai, ESS

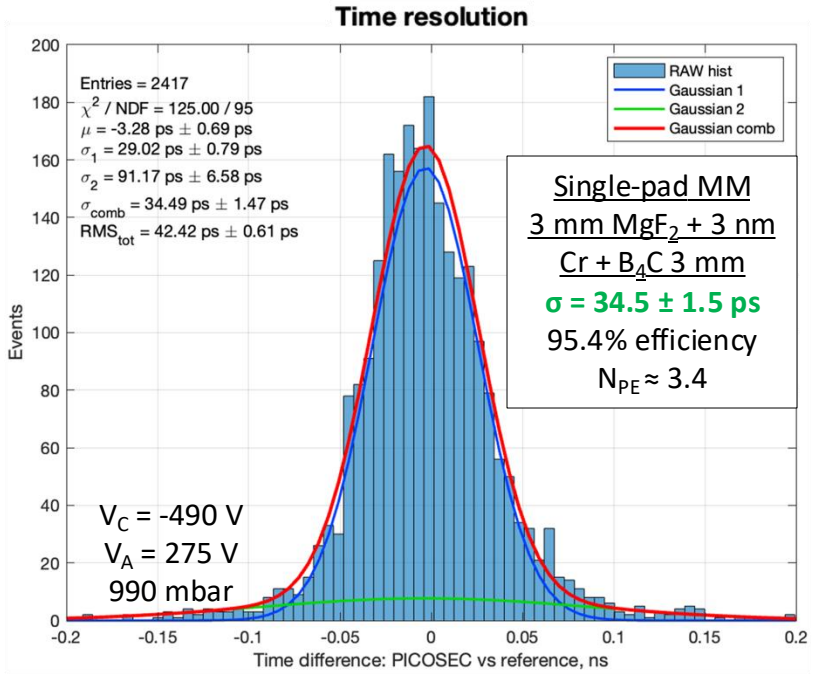

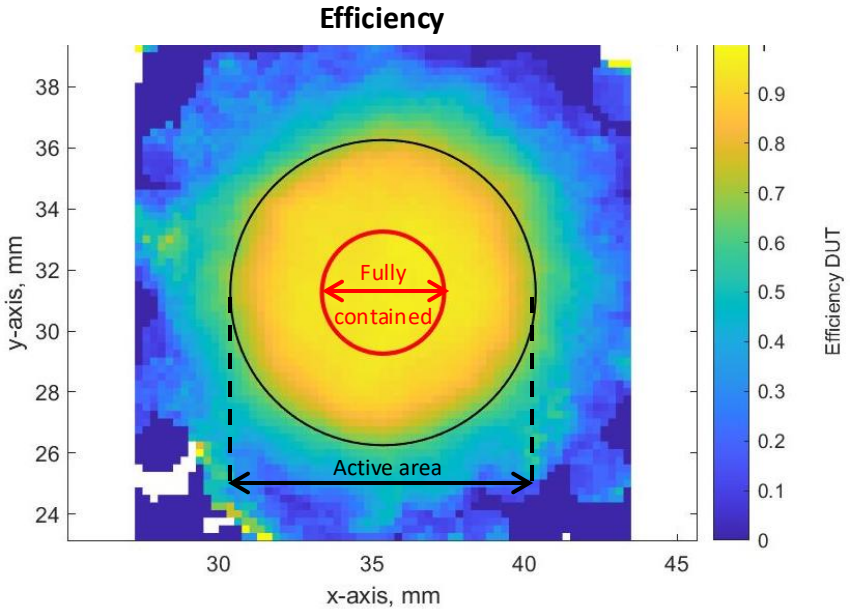

M. Lisowska et al., arXiv:2407.09953

Photocathode characterisation

Titanium as a conductive interlayer

- The MgF_2 substrate exhibits 80% transparency @180 nm, it decreases to 45% with adding the Cr layer and drops to 10% with the CsI
- The 35% reduction in transparency after adding the Cr layer is primarily due to light absorption, which diminishes the number of photons reaching the photocathode → This issue could be mitigated by using a different contact material with better transparency
- Titanium (Ti) is the most favourable candidate, with ~15% higher transparency compared to Cr

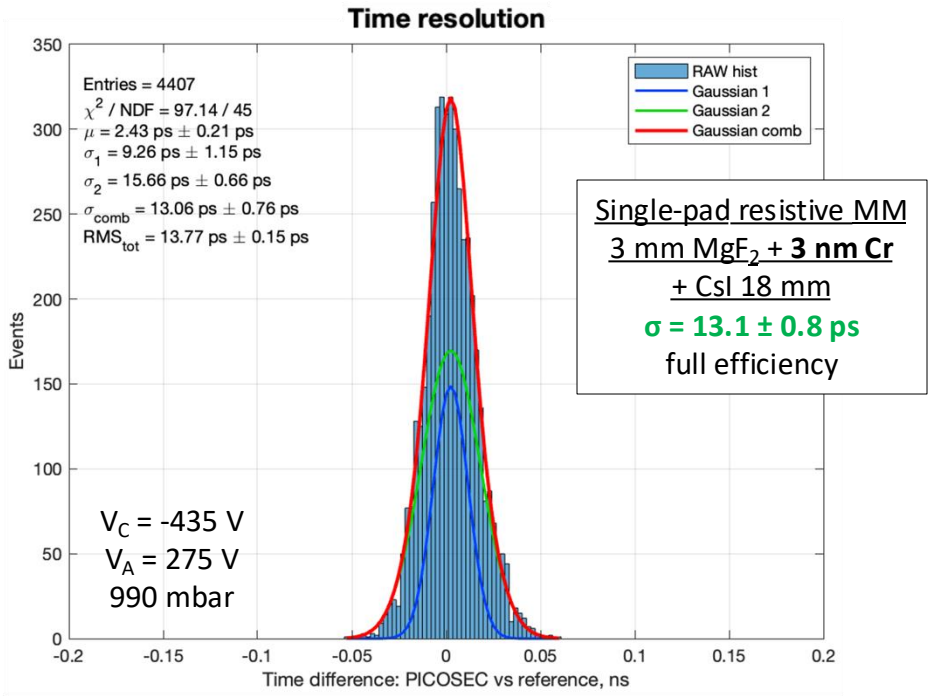

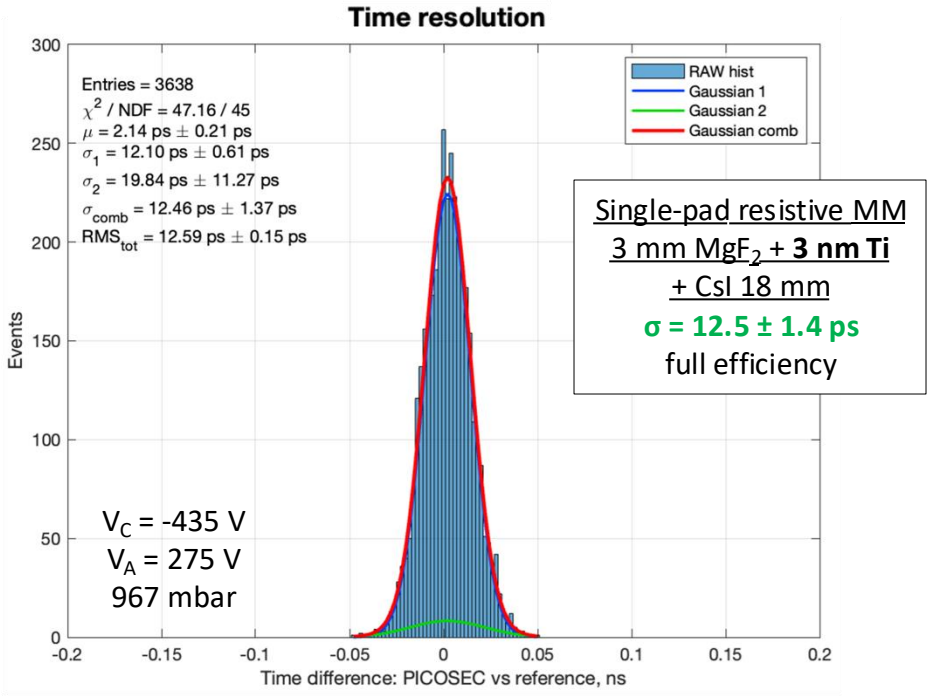

Photocathode characterisation

Graphene as a protective layer

- In studies using graphene as a photocathode, a 2.5–3 nm Ti layer produced $N_{PE} \approx 4.3$ and showed a time resolution $\sigma < 30$ ps
- Adding graphene partially screens the photoelectron (PE) emission from the Ti, with the monolayer (ML) screening ~30% and the bilayer (BL) and trilayer (TL) screening ~50% of the PEs → time resolution down to $\sigma \approx 36$ ps for Ti + a ML of graphene
- Graphene could be considered as a protective layer

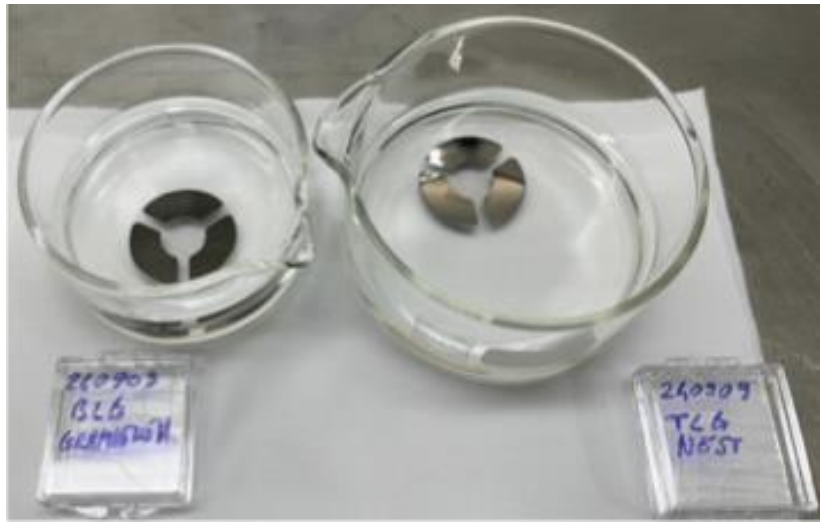

Graphene photocathodes with varying layer number, G. Orlandini

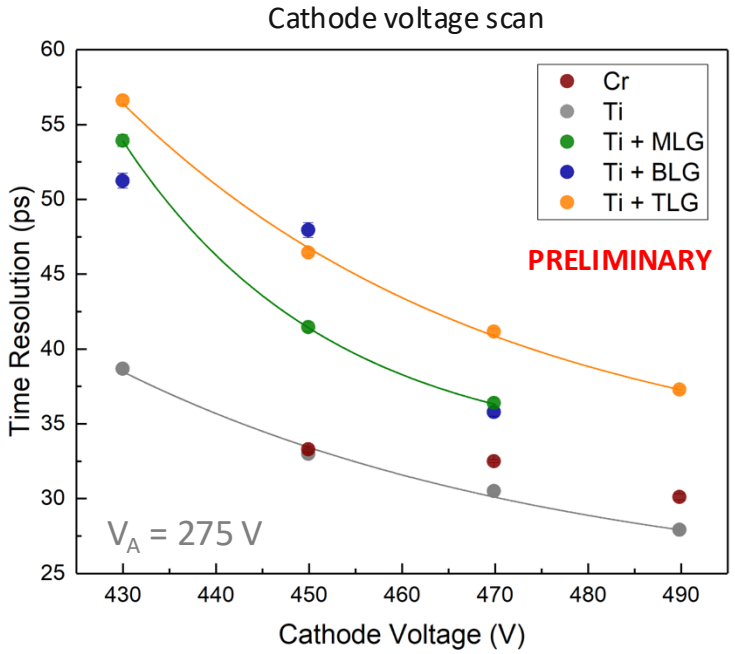

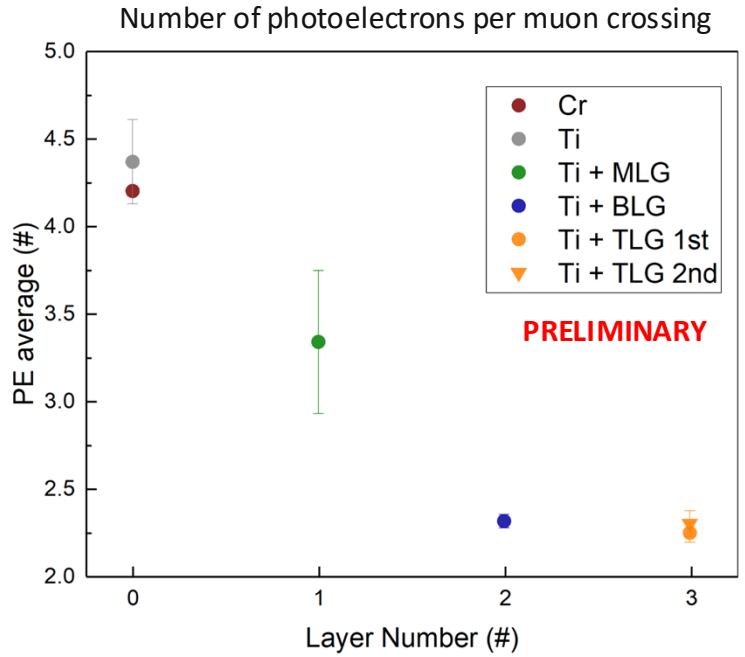

Photocathode characterisation

Sensitivity to humidity

- Photocathodes with Cr + CsI show traces of no CsI with accumulation of the material at the ends
- Photocathodes with Ti + CsI also show traces of no CsI but without accumulation dots of the material
- Both DLC and B_4C photocathodes have uniform layers with some scratches on the top, most likely due to the sample handling

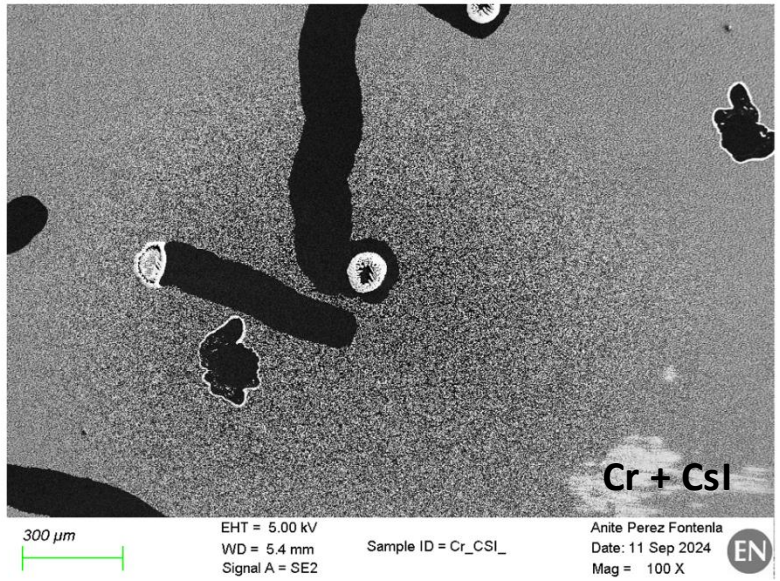

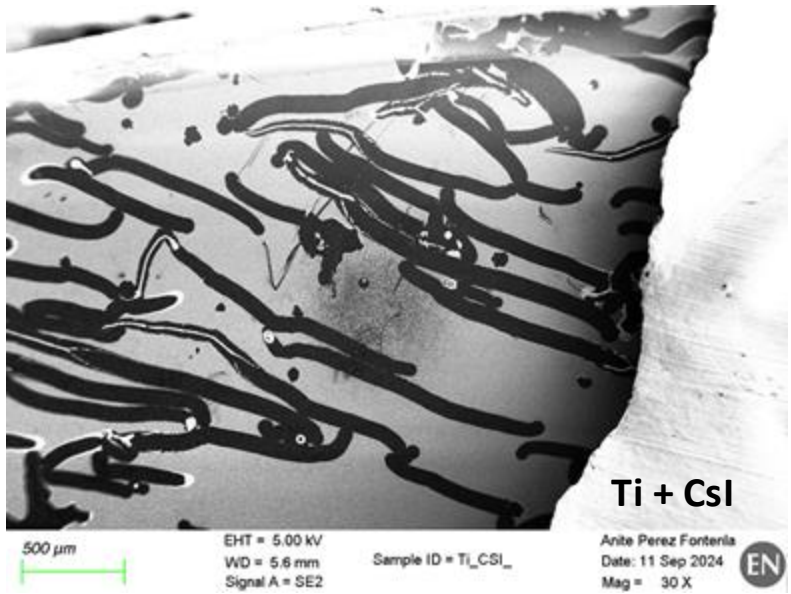

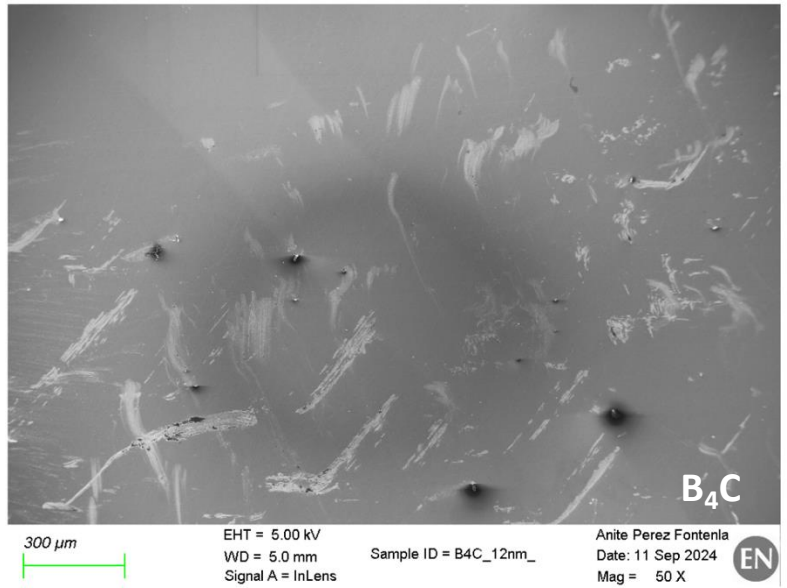

Towards applicable detector

Stable and robust prototype

- First measurement combining a single-pad 15 mm dia. **resistive Micromegas, a DLC photocathode and an amplifier embedded into the outer PCB** showed stable performance and achieved a **time resolution of σ = 31.4 ± 0.6 ps**, capturing fully contained events

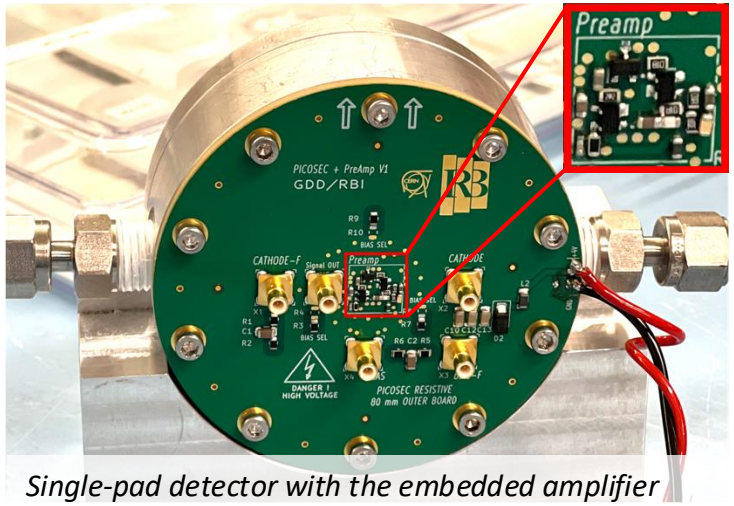

Single-pad detector with the embedded amplifier

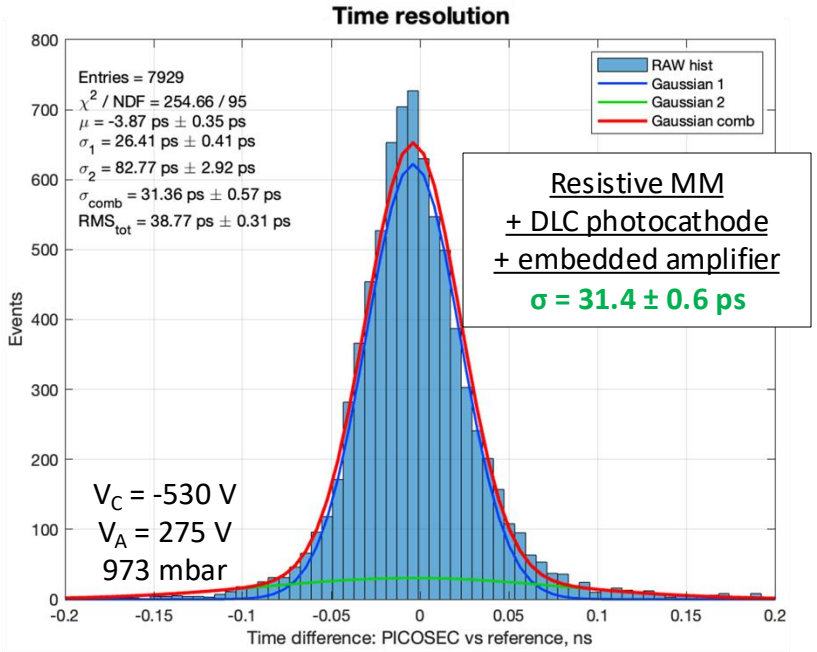

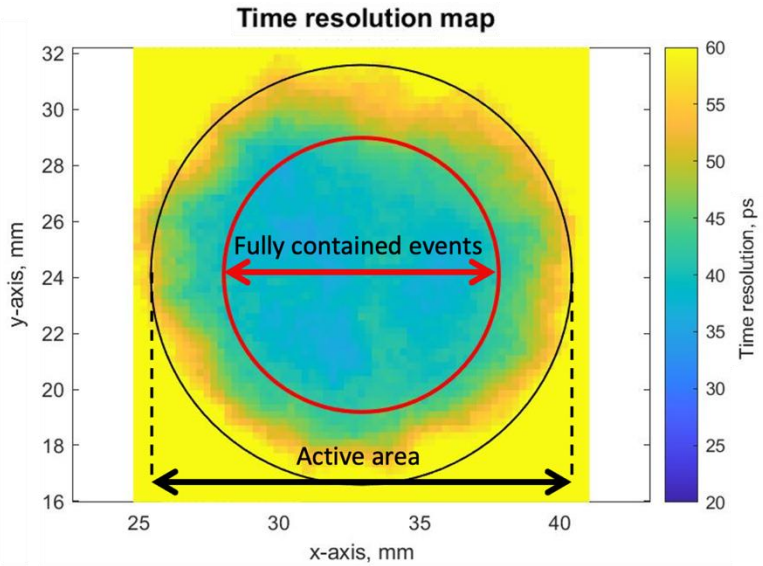

M. Lisowska et al., arXiv:2407.09953

Towards applicable detector

100-channel module performance

- Several pads of the 100-channel module were characterised during particle beam measurements with an oscilloscope
- Prototype equipped with a **CsI photocathode** achieved a **time resolution of σ ≈ 18 ps**
- Detector assembled with a **DLC photocathode** obtained a **time resolution of σ ≈ 35 ps**
- First measurements with a **B_4C photocathode** showed a **time resolution of σ ≈ 41 ps**

} for individual pads and fully contained events

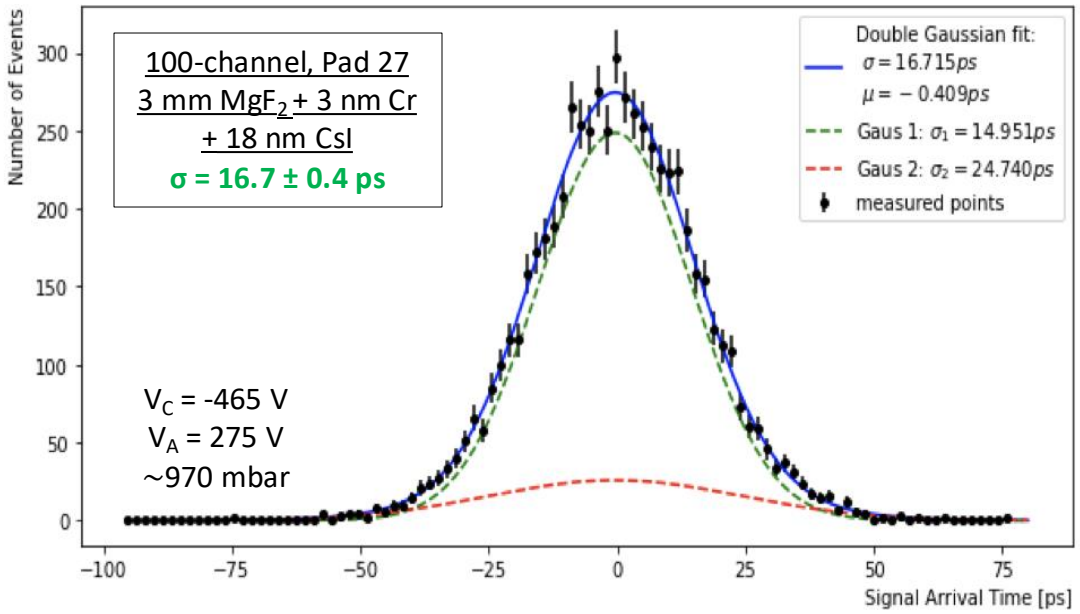

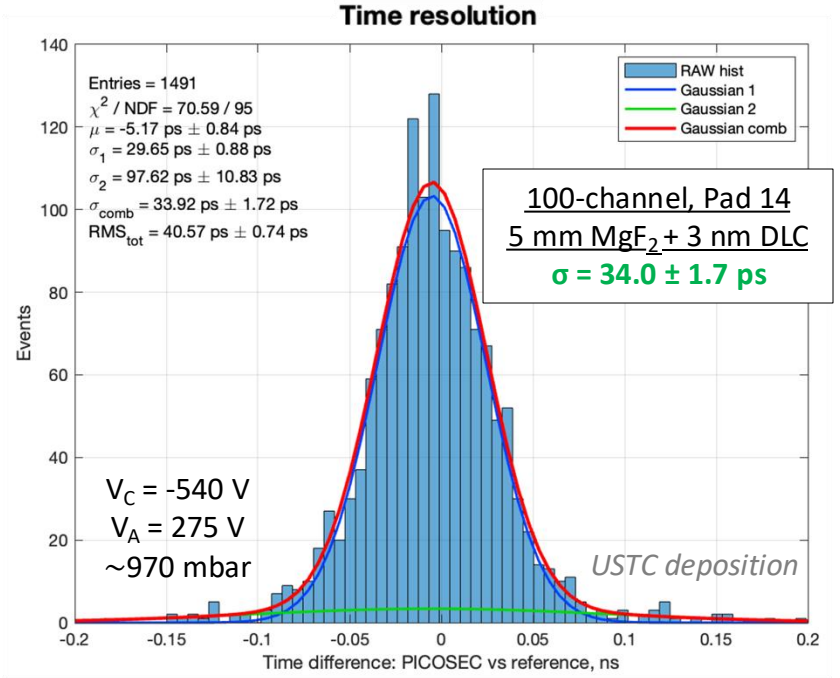

E. Chatzianagnostou, MSc thesis (2022)

Conclusions

- **Intensive studies on robust photocathodes** resulted in achieving great time resolutions of σ ≈ 32 for DLC, σ ≈ 34.5 ps for B_4C and σ ≈ 36 ps for Ti + a ML of graphene photocathodes
- Carbon-based materials displayed notably greater resistance to discharges and humidity and have been reused across multiple test beam campaigns, showing no deterioration in time resolution
- Measurements confirmed that the excellent timing can be transferred to a 100-channel module, achieving σ ≈ 18 ps for CsI, σ ≈ 35 ps for DLC and σ ≈ 41 ps for B_4C photocathodes
- **The efforts dedicated to advancing the detectors increase the feasibility of the PICOSEC concept for experiments requiring sustained performance while maintaining excellent timing precision**

Future perspectives

- Ageing studies of the DLC and B_4C, response to IBF
- Deposition of the B_4C and a mix of DLC+B_4C photocathodes at the CERN MPT workshop
- Production of 10x10 cm^2 area robust photocathodes at the CERN MPT workshop
- Search for other alternative materials (carbon nano-structures, nanodiamonds – low efficiency)

PICOSEC Micromegas Collaboration

M. Lisowska[1,2,*], Y. Angelis[3], J. Bortfeldt[4], F. Brunbauer[1], E. Chatzianagnostou[3], K. Dehmelt[5], G. Fanourakis[6], K. J. Floethner[1,7], M. Gallinaro[8], F. Garcia[9], P. Garg[5], I. Giomataris[10], K. Gnanvo[11], T. Gustavsson[12], F.J. Iguaz[10], D. Janssens[1,13,14], A. Kallitsopoulou[10], M. Kovacic[15], P. Legou[10], J. Liu[16], M. Lupberger[7,17], S. Malace[11], I. Maniatis[1,3], Y. Meng[16], H. Muller[1,17], E. Oliveri[1], G. Orlandini[1,18], T. Papaevangelou[10], M. Pomorski[19], L. Ropelewski[1], D. Sampsonidis[3,20], L. Scharenberg[1,17], T. Schneider[1], L. Sohl[10], M. van Stenis[1], Y. Tsipolitis[21], S.E. Tzamarias[3,20], A. Utrobicic[22], R. Veenhof[1,23], X. Wang[16], S. White[1,24], Z. Zhang[16], and Y. Zhou[16]

[1]European Organization for Nuclear Research (CERN), CH-1211, Geneve 23, Switzerland
[2]Université Paris-Saclay, F-91191 Gif-sur-Yvette, France
[3]Department of Physics, Aristotle University of Thessaloniki, University Campus, GR-54124, Thessaloniki, Greece
[4]Department for Medical Physics, Ludwig Maximilian University of Munich, Am Coulombwall 1, 85748 Garching, Germany
[5]Stony Brook University, Dept. of Physics and Astronomy, Stony Brook, NY 11794-3800, USA
[6]Institute of Nuclear and Particle Physics, NCSR Demokritos, GR-15341 Agia Paraskevi, Attiki, Greece
[7]Helmholtz-Institut für Strahlen- und Kernphysik, University of Bonn, Nußallee 14–16, 53115 Bonn, Germany
[8]Laboratório de Instrumentacão e Física Experimental de Partículas, Lisbon, Portugal
[9]Helsinki Institute of Physics, University of Helsinki, FI-00014 Helsinki, Finland
[10]IRFU, CEA, Université Paris-Saclay, F-91191 Gif-sur-Yvette, France
[11]Jefferson Lab, 12000 Jefferson Avenue, Newport News, VA 23606, USA
[12]LIDYL, CEA, CNRS, Universit Paris-Saclay, F-91191 Gif-sur-Yvette, France
[13]Inter-University Institute for High Energies (IIHE), Belgium
[14]Vrije Universiteit Brussel, Pleinlaan 2, 1050 Brussels, Belgium
[15]Faculty of Electrical Engineering and Computing, University of Zagreb, 10000 Zagreb, Croatia
[16]State Key Laboratory of Particle Detection and Electronics, University of Science and Technology of China, Hefei 230026, China
[17]Physikalisches Institut, University of Bonn, Nußallee 12, 53115 Bonn, Germany
[18]Friedrich-Alexander-Universität Erlangen-Nürnberg, Schloßplatz 4, 91054 Erlangen, Germany
[19]CEA-LIST, Diamond Sensors Laboratory, CEA Saclay, F-91191 Gif-sur-Yvette, France
[20]Center for Interdisciplinary Research and Innovation (CIRI-AUTH), Thessaloniki 57001, Greece
[21]National Technical University of Athens, Athens, Greece
[22]Institute Ruder Bosković Institute, Bijenička cesta 54, 10000, Zagreb, Croatia
[23]Bursa Uludağ University, Görükle Kampusu, 16059 Niufer/Bursa, Turkey
[24]University of Virginia, USA

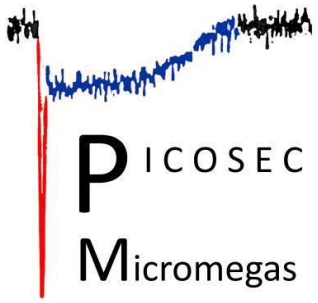

Thank you for your attention!

CONTACT: MARTA.LISOWSKA@CERN.CH

Back up slides

PICOSEC Micromegas

Pre-amplification gap

- Higher electric field → Early avalanche → **Reduced Signal Arrival Time (SAT)**
- Thinner pre-amplification gap limits the direct ionisation and grants a stable operation

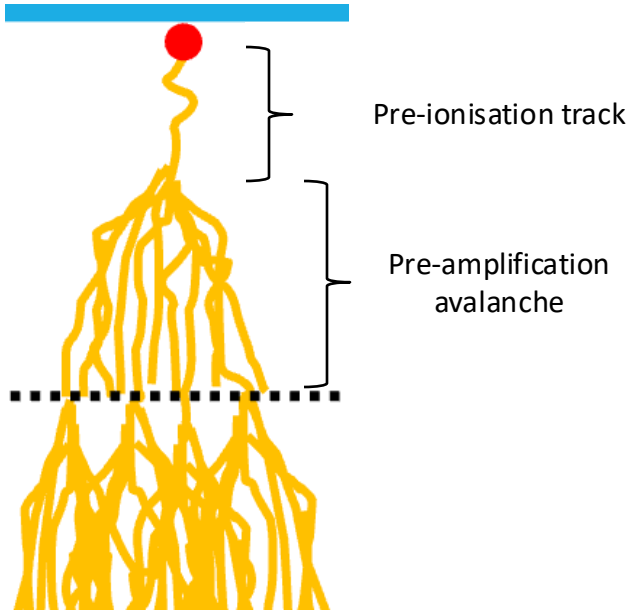

Garfield++ simulations

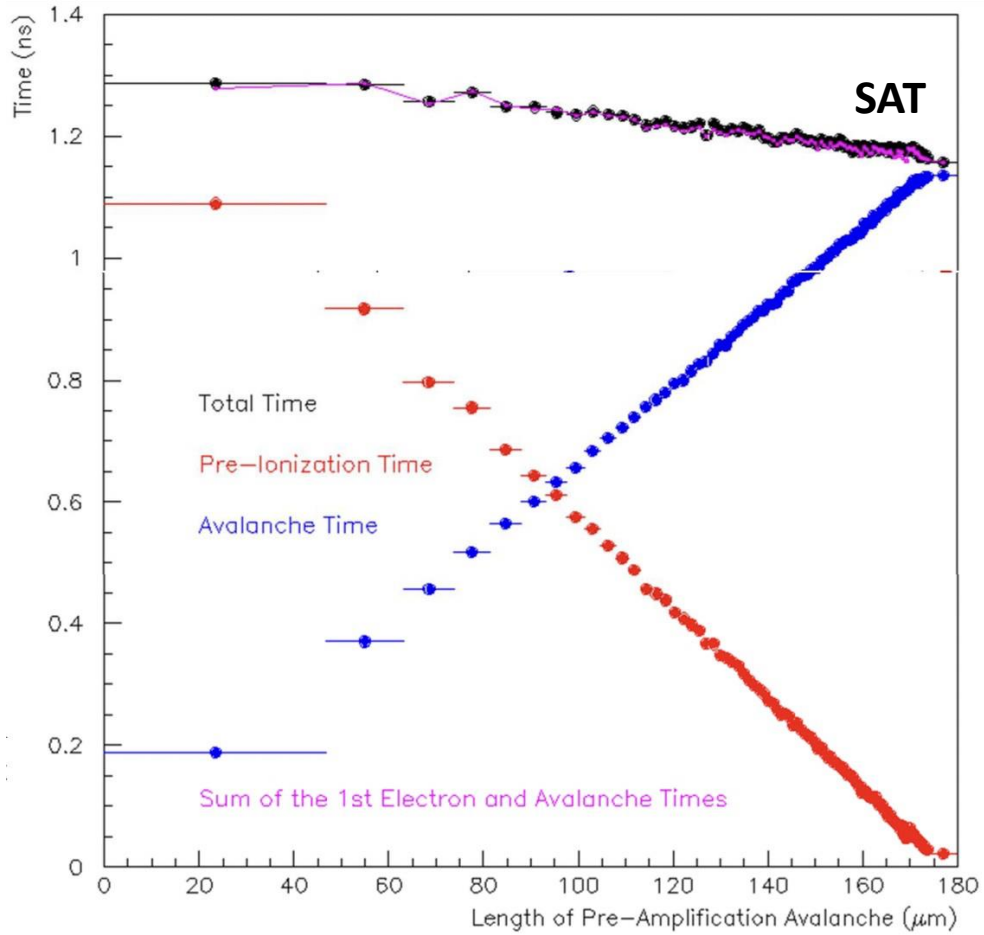

J. Bortfeldt et al., NIM A 993 (2021) 165049

Photocathode characterisation

QE measurements - Reflective mode

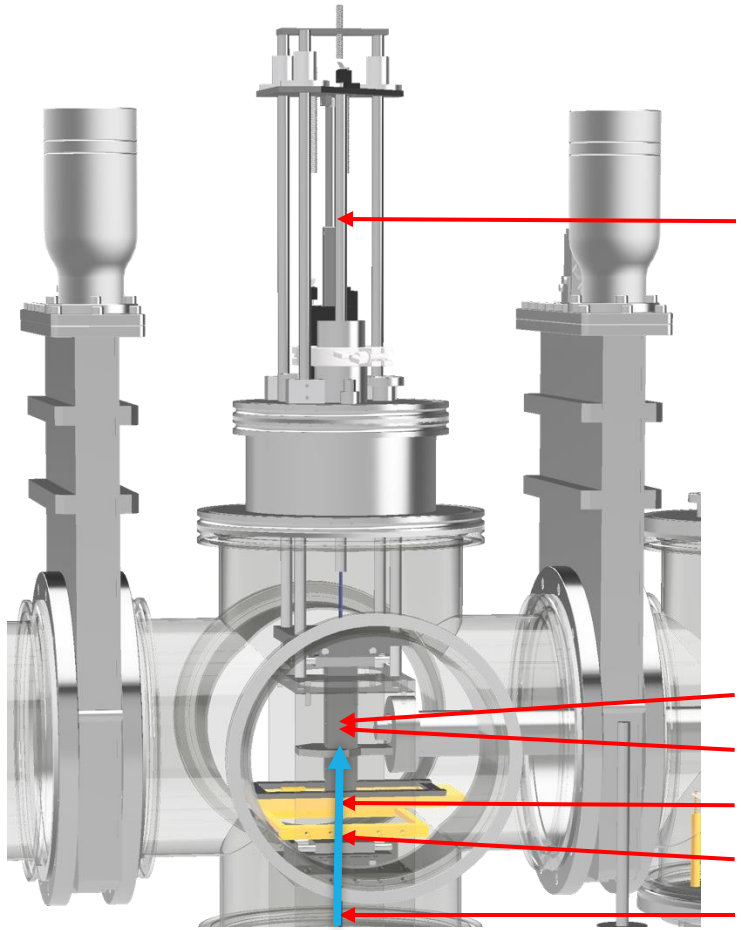

$$QE = \frac{N_e}{N_{ph}} = \frac{\frac{I_s}{e}}{\frac{I_{PMT}}{e \cdot C_{PMT}}} = \frac{I_s \cdot C_{PMT}}{I_{PMT}}$$

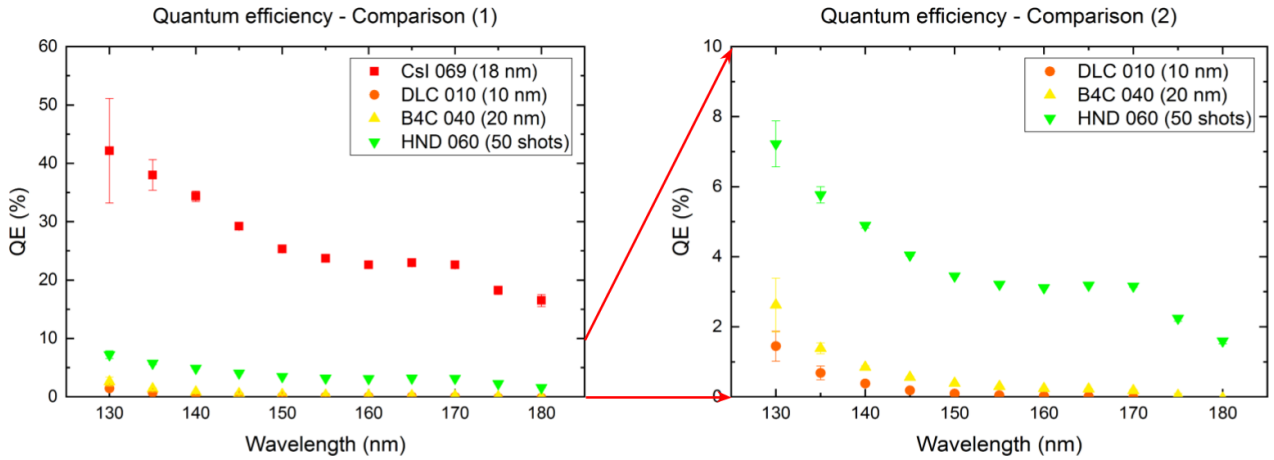

Photocathode characterisation

QE measurements - Transmission mode

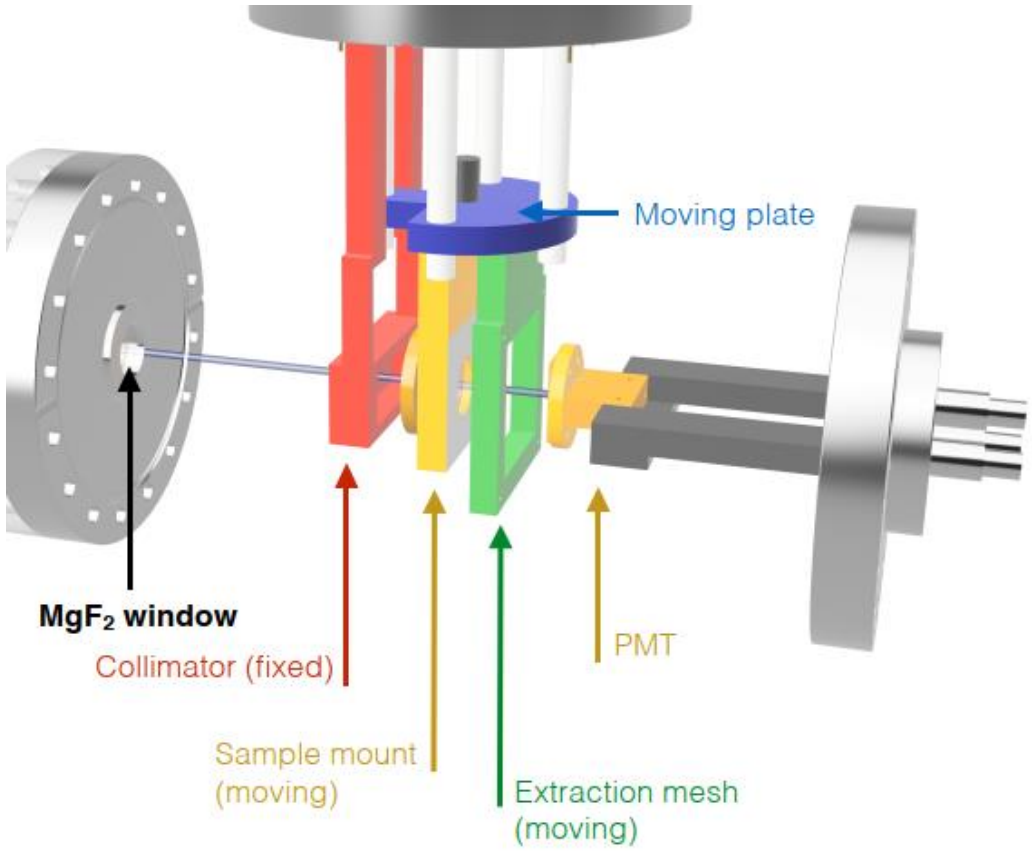

$$QE = \frac{N_e}{N_{ph}} = \frac{\frac{I_s}{e}}{\frac{I_{PMT}}{e \cdot C_{PMT}}} = \frac{I_s \cdot C_{PMT}}{I_{PMT}}$$

$$T = \frac{I_{PMT,\ s.\ in}}{I_{PMT,\ s.\ out}}$$

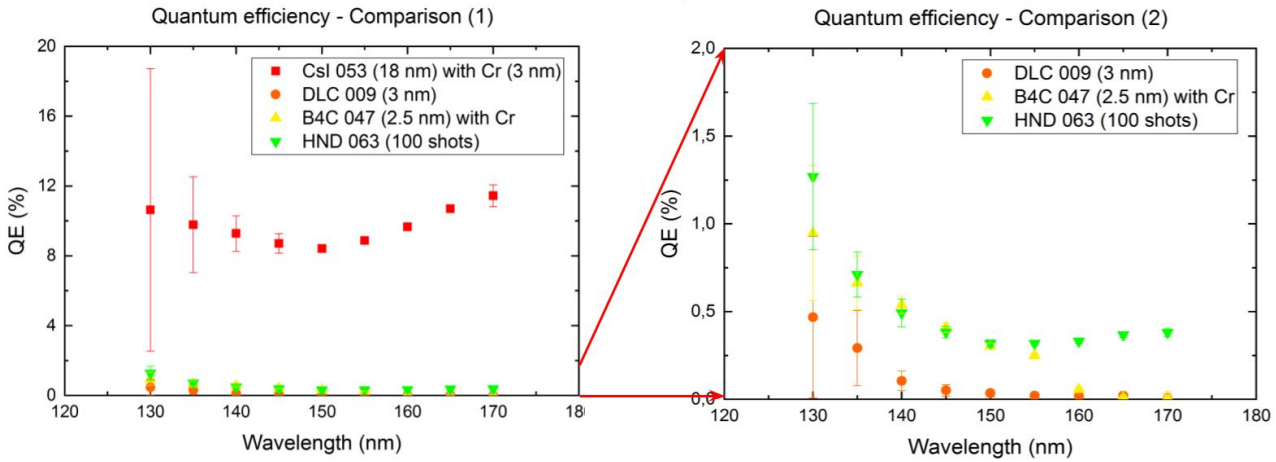

Photocathode characterisation

Ageing studies – Irradiation mode

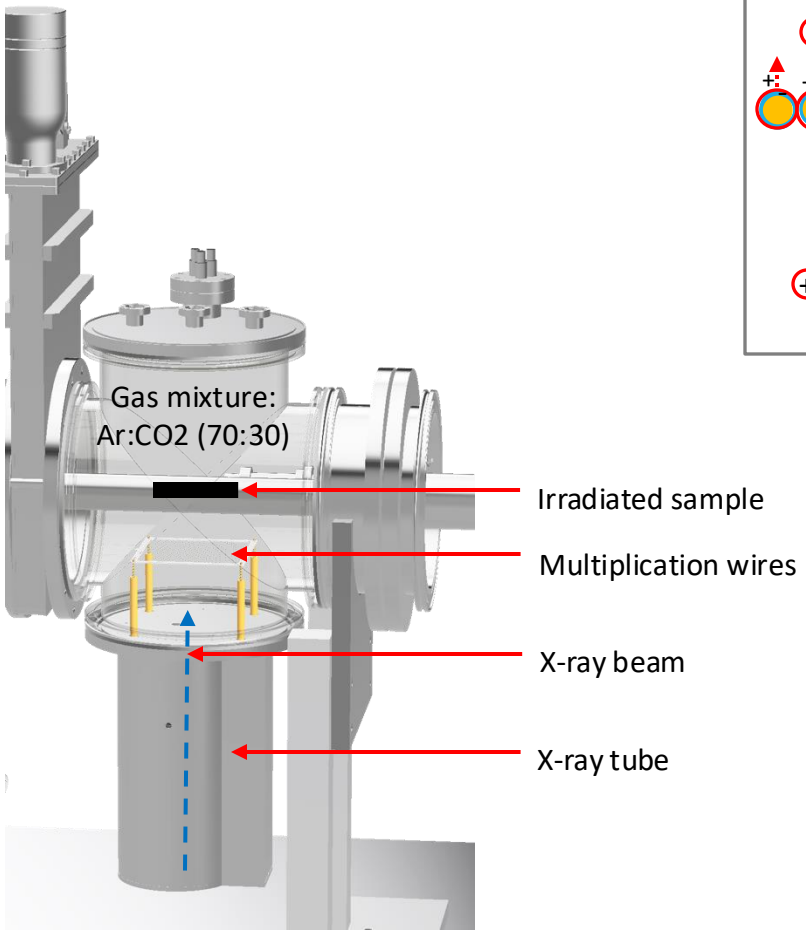

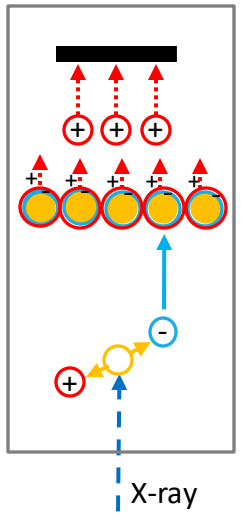

3. Irradiated sample (grounded):
Attraction of ions from avalanche
Accumulation of charge

2. Multiplication wires (positive HV):
Attraction of primary electrons
Avalanche multiplication
Production of electrons and ions

1. X-ray beam in a gas chamber:
Ionization of particles
Creation of primary charge

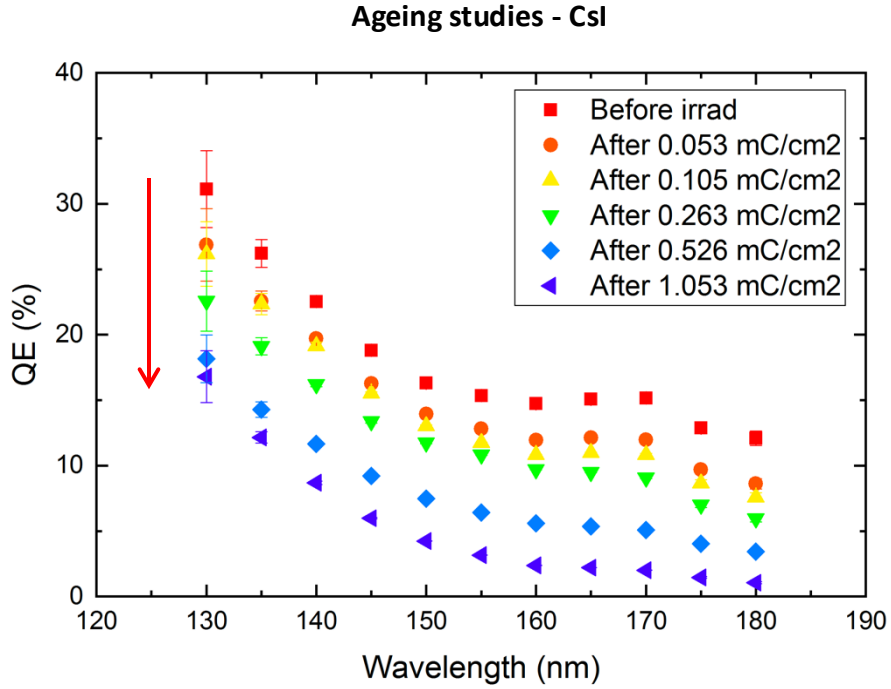

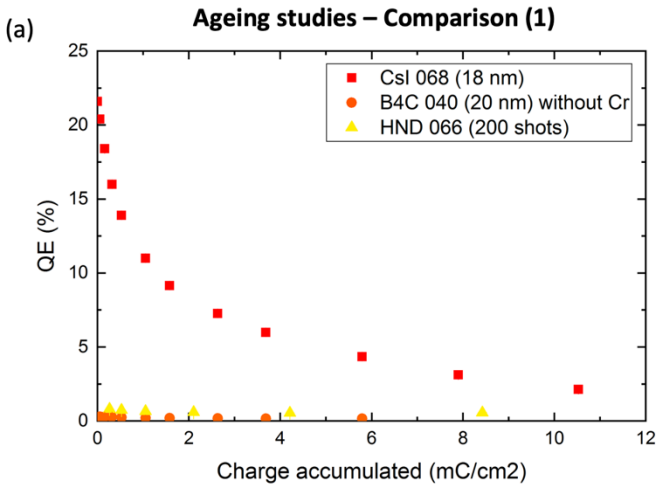

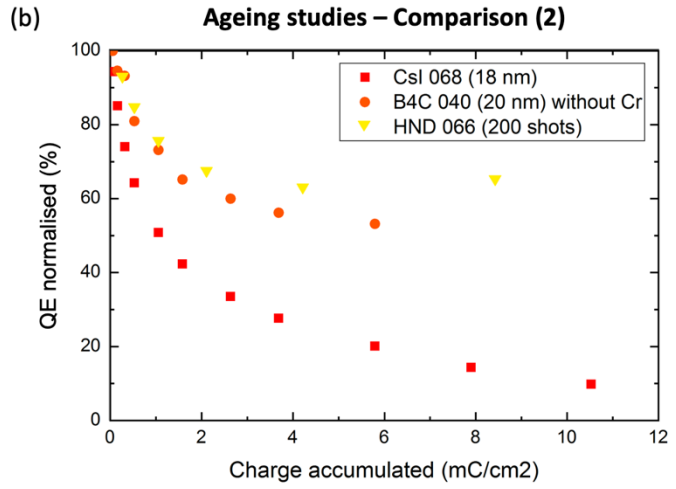

PICOSEC Micromegas

Signal analysis

- Quantifying the PICOSEC detector's time resolution requires a reference device with a superior timing precision: MCP-PMT $\sigma_{MCP} \approx 6$ ps
- Leading edge of the signal fitted using a sigmoid function - timestamps determined at 20% of the signal amplitude (CFD method)
- Signal Arrival Time (SAT) computed as a difference between the timestamps: SAT = $t_{PICO} - t_{MCP}$
- The histogram of SAT values fitted with a double Gaussian function
- Time resolution - standard deviation of the SAT distribution

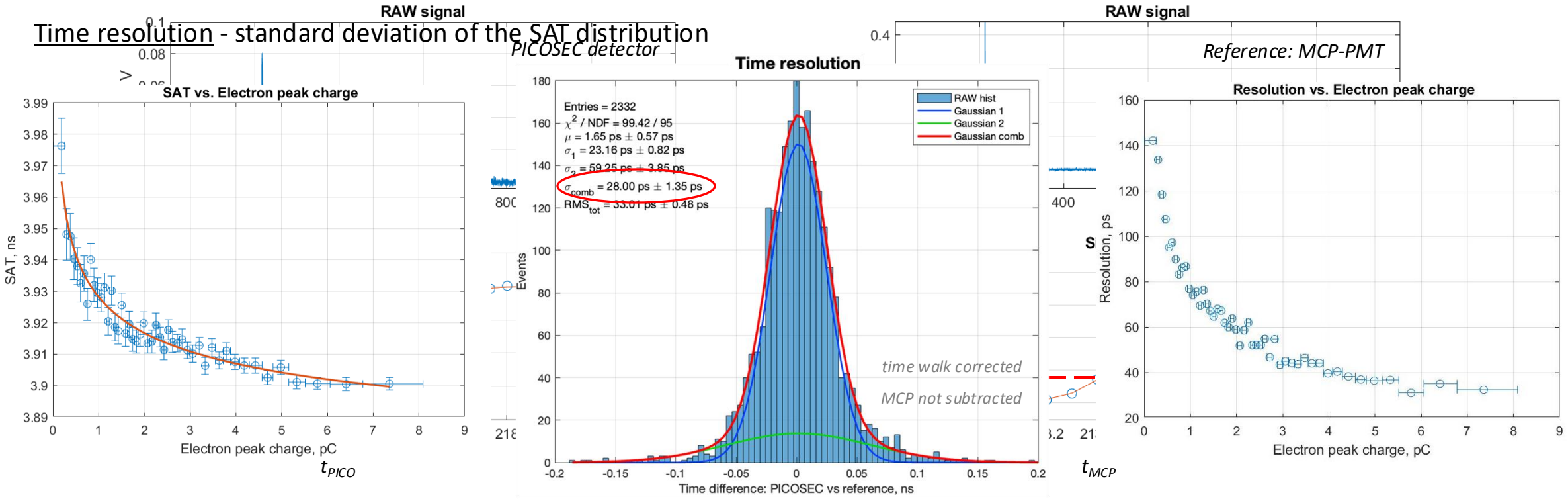

PICOSEC Micromegas

Double Gaussian function

The histogram of SAT values was fitted with a double Gaussian function, which effectively approximates the shape of the distribution and accounts for the variations between the SAT and the e-peak charge. The double Gaussian function is given by the equation

$$f(\Delta t) = N\left[a\, exp\left(-\frac{\Delta t-\mu}{2\sigma_{core}^2}\right) + (1-a)\, exp\left(-\frac{\Delta t-\mu}{2\sigma_{tail}^2}\right)\right],$$

where N is a scaling factor, $a \in [0,1]$ is a weighting parameter, μ is the mean of the distribution, σ_{core} is the standard deviation of the core Gaussian, and σ_{tail} is the standard deviation of the Gaussian describing the tail. The weighting parameter between the two Gaussian components enables the determination of the combined standard deviation σ_{comb}^2 of the overall distribution:

$$\sigma_{comb}^2 = a\,\sigma_{core}^2 + (1-a)\,\sigma_{tail}^2.$$

This combined standard deviation σ_{comb}^2 represents the time resolution of the detector system.

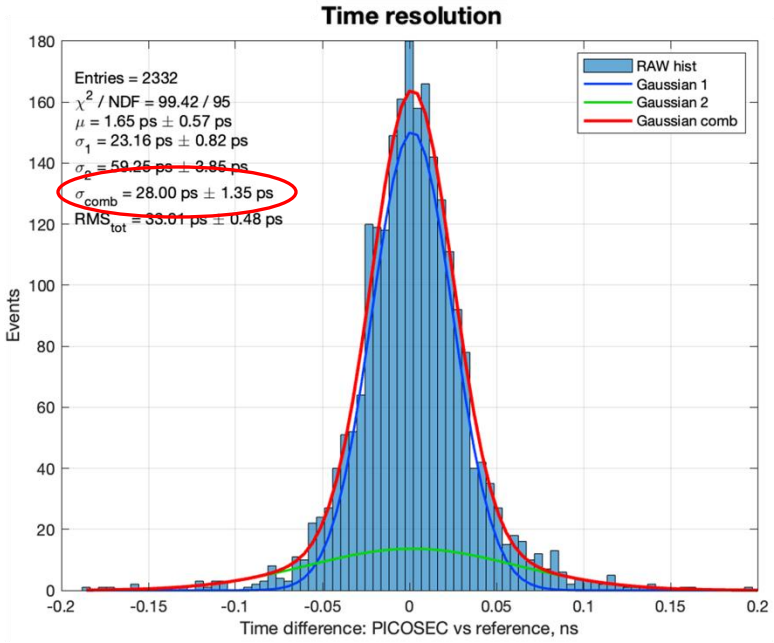

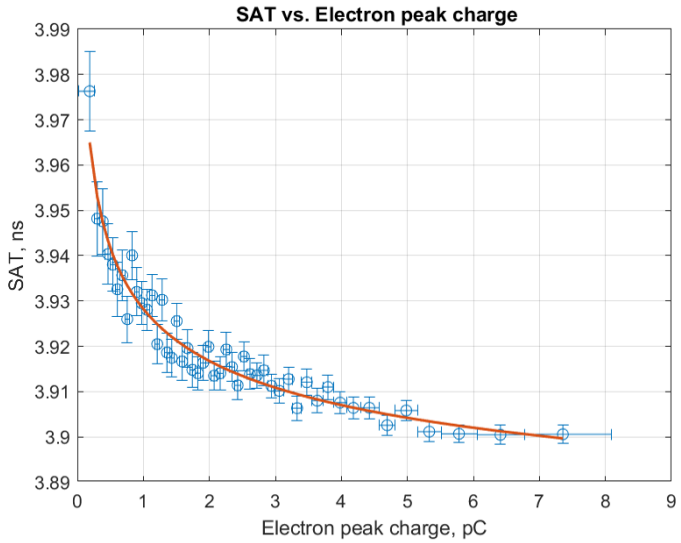

PICOSEC Micromegas

Signal analysis

- In addition to time resolution, several other parameters are evaluated and compared across the prototypes

Signal spectrum for a PICOSEC detector and an MCP-PMT with a mean max amplitude to compare the gain and homogeneity

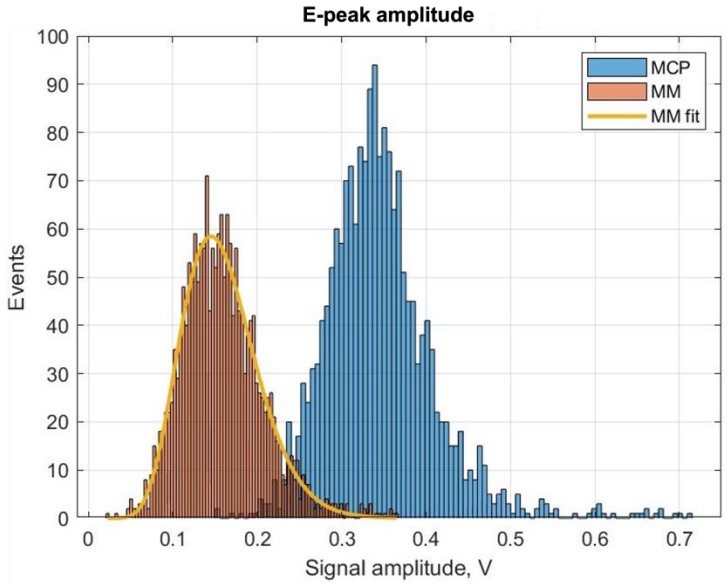

Rise time of the leading edge 10-90 % of max amplitude to see the influence of capacitance

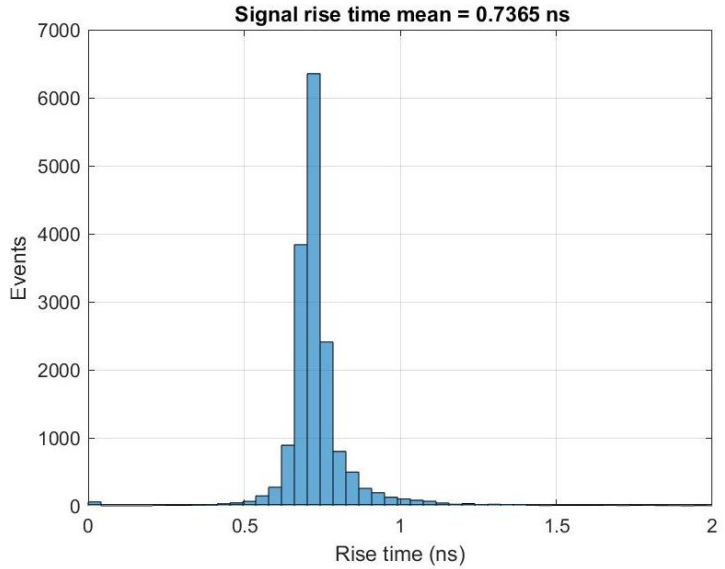

Detection efficiency depending on N_{PE}

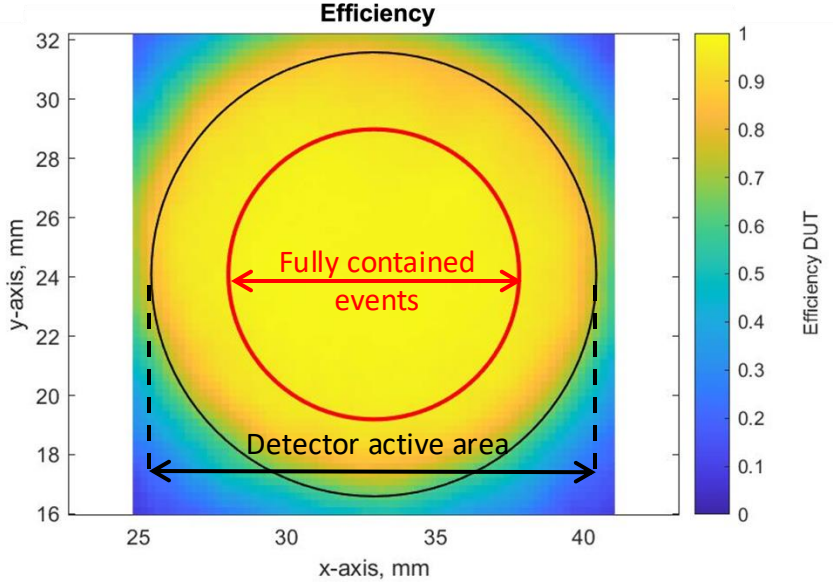

All reported results concern fully contained events due to the Cherenkov cone

Photocathode characterisation

Nanodiamonds

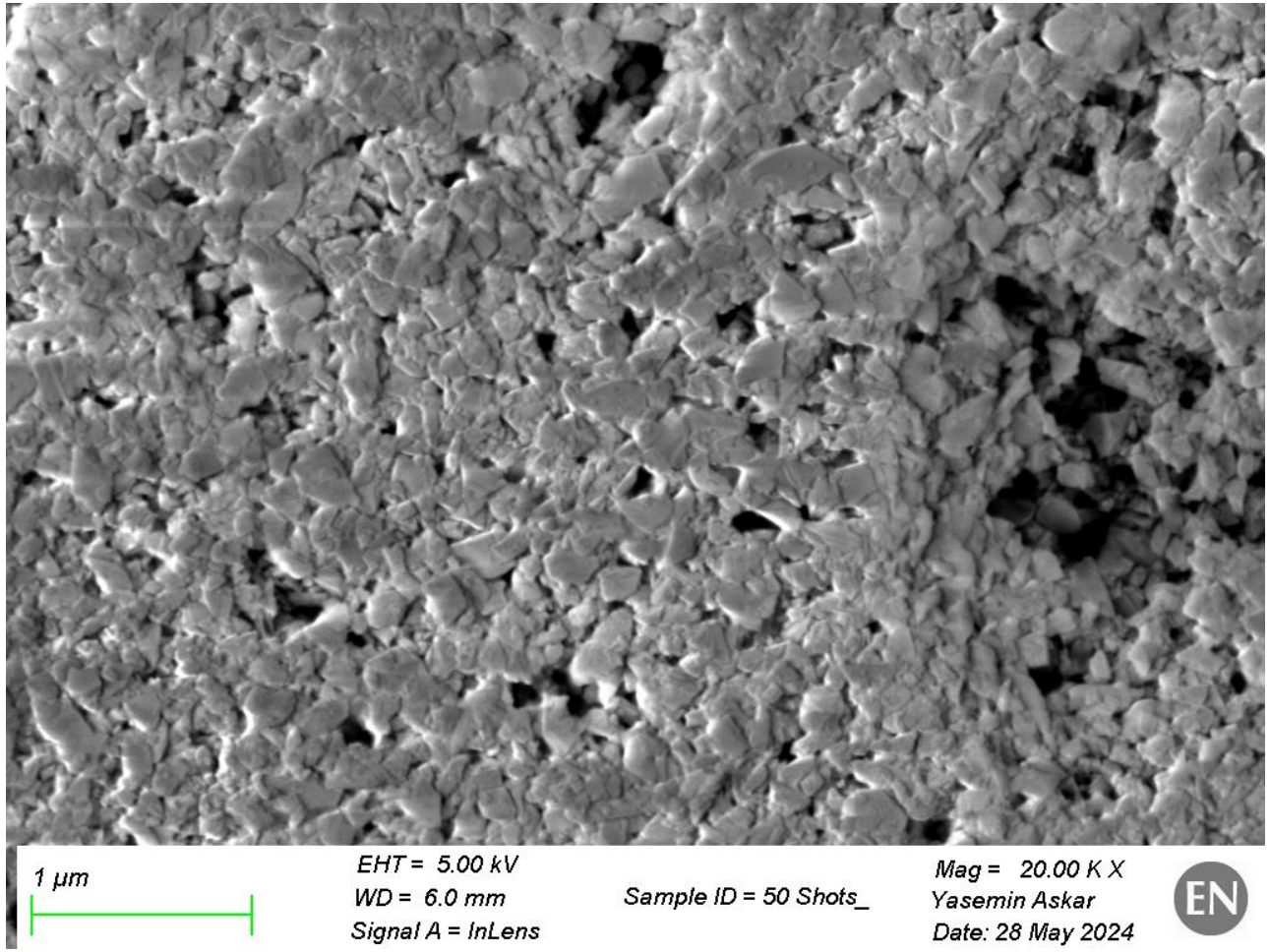

Large-area coverage

100-channel module design

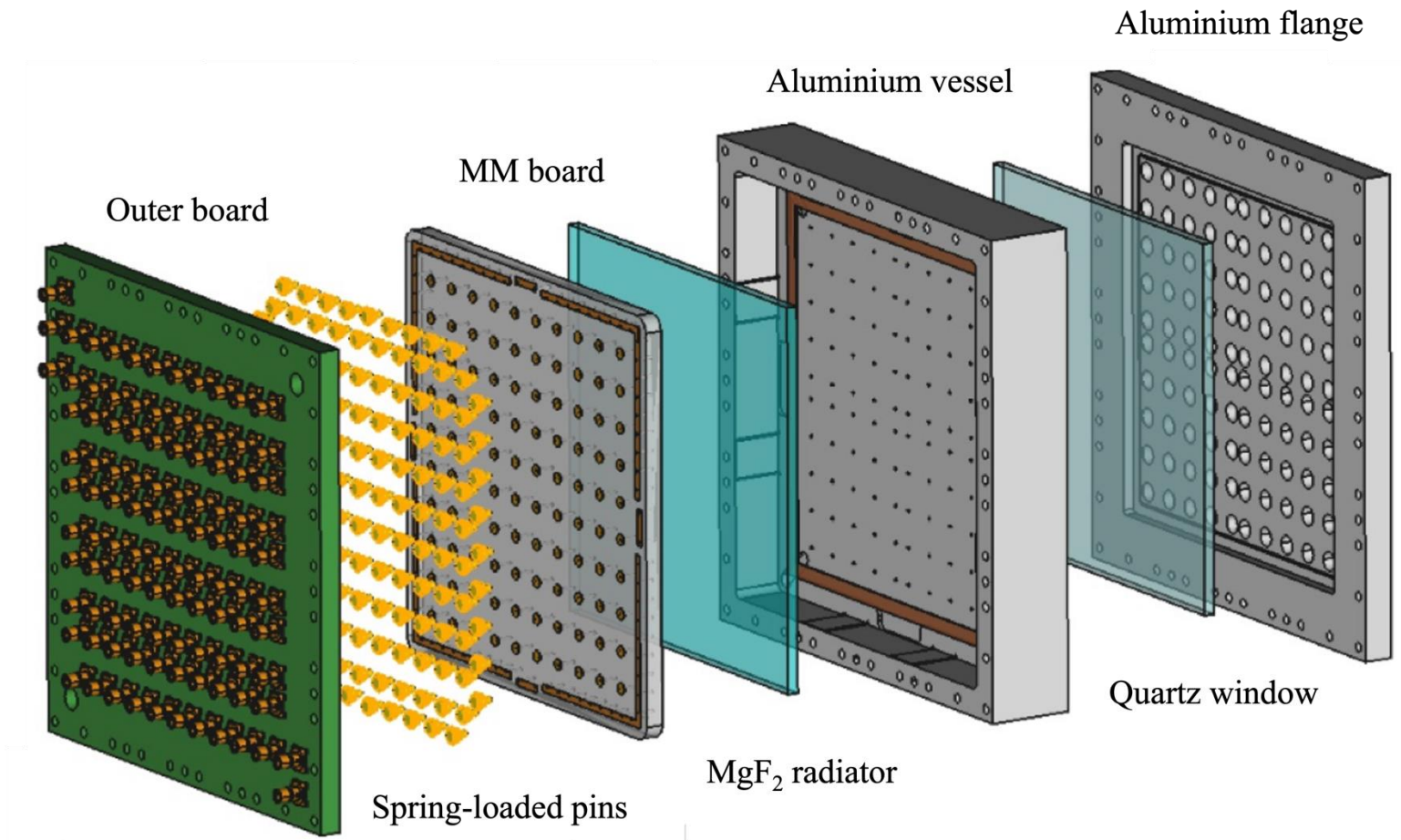

PICOSEC amplifier cards

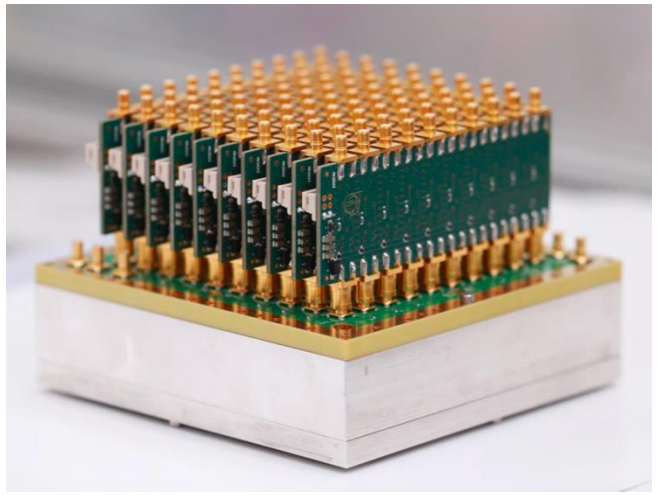

A. Utrobičić, et al. JINST 18 (2023) C07012

LeCroy WR8104 oscilloscope or
SAMPIC Waveform TDC

D. Breton et al., NIM A 835 (2016) 51